

ABSTRACT

HONG, KI. Development and Characterizations of Two-Dimensional Heterogeneous Catalysts for Transesterification Reactions. (Under the direction of Dr. Wei Gao).

Novel heterogeneous catalysts that are capable of catalyzing transesterification reactions and later being separated from the reaction products are developed and characterized in this study. Graphene oxide (GO) and MXene (MX), both as representative nanoscale two-dimensional sheets, are used as supporting matrices on which the catalytic species are attached. The conventional dibutyltin oxide catalyst was grafted onto the surfaces of the two matrices, and the resulted heterogeneous catalysts have been characterized on their compositional, morphological, and catalytic features. Namely GO-Sn and MX-Sn, both heterogeneous catalysts have been applied in transesterification reactions between dimethyl terephthalate (DMT) and 2,2,4,4-tetramethyl-1,3-cyclobutanediol (TMCD), with over 90% DMT conversions observed in both cases. Prioritizing GO-Sn as the main subject for further investigations, the separability and reusability of the GO-Sn catalyst have been explored in our lab-scale vacuum filtration processes. Despite varying levels of tin leaching from the 2D matrices, GO-Sn can be reasonably separated from the oligomer products using solvents like tetrahydrofuran (THF). Reversible tin leaching upon extended reaction time is also observed. In addition, our GO-Sn catalyst turns out to be highly effective in reactions between DMT and other diol reactants (neopentyl glycol, 2-methyl-1,3-propanediol, and 1, 4-cyclohexanedimethanol), indicating a broadened scope of applications and practicality for industrial-scale reactions.

© Copyright 2021 by Ki Hong

All Rights Reserved

Development and Characterizations of Two-Dimensional Heterogeneous Catalysts
for Transesterification Reactions

by
Ki Hong

A thesis submitted to the Graduate Faculty of
North Carolina State University
in partial fulfillment of the
requirements for the degree of
Master of Science

Textile Chemistry

Raleigh, North Carolina
2021

APPROVED BY:

Dr. Wei Gao
Committee Chair

Dr. Richard Kotek

Dr. Christopher Gorman

DEDICATION

To mother, who selflessly provides;

To sister, who relentlessly supports;

And to father, who endlessly loves.

BIOGRAPHY

Ki Hong is originally from Seoul, South Korea, and he continued his academic studies in United States to obtain his Bachelor of Science in *Polymer and Color Chemistry: Medical Science Concentration* and a minor in *Biological Sciences* at *North Carolina State University* on May 2017. Later, he joined to pursue a master's degree in *Textile Chemistry* at *North Carolina State University* on August 2019, and worked on a collaborative project with *Eastman Chemical Company* under the supervision of Dr. Wei Gao.

ACKNOWLEDGMENTS

First and foremost, I would like to express my sincere appreciation and gratitude to my advisor, Dr. Wei Gao, for guiding and supporting me throughout my research. She was always available to provide both insightful advice and friendly conversations that I deeply treasure as an invaluable relationship and memorable experience of my graduate studies.

I would also like to extend my gratitude to the associates of Eastman Chemical Company for providing such an incredible opportunity to work on the project. Not only did I learn a lot from the research itself, but I also got to learn more about myself and interest for scientific research.

Moreover, I would like to show my appreciation to Dr. Richard Kotek and Dr. Christopher Gorman for being my committee members and their contributions to my thesis work.

I would like to thank Dr. Shradha Patil for her contributions to the earlier portion of this research up to the preliminary tests, and Dr. Nanfei He for her aids in the lab and characterization work. I also treasure the moments not only as colleagues but also as friends.

I am very thankful and glad to build relationships with other colleagues and friends I have met throughout the graduate journey, as they have provided kind support and encouragement amidst the hardships, especially during the COVID-19 pandemic.

Last but not least, I am very grateful for the research facilities and resources provided from the Wilson College of Textiles; Molecular Education, Technology and Research Innovation Center (METRIC); Analytical Instrumentation Facility (AIF); and Chemical Analysis and Spectroscopy Laboratory (CASL); all located at North Carolina State University.

TABLE OF CONTENTS

LIST OF TABLES	vi
LIST OF FIGURES	vii
CHAPTER 1: Introduction	1
1.1 Backgrounds	1
1.2 Objectives	1
CHAPTER 2: Literature Review	3
2.1 Homogeneous Catalyst	3
2.2 Heterogeneous Catalyst	8
2.3 Two-Dimensional Matrix Catalyst	13
CHAPTER 3: Experiments and Discussion	17
3.1 Synthesis of 2D Heterogeneous Catalysts	17
3.2 Preliminary Characterizations of 2D Heterogeneous Catalysts	20
3.3 Transesterification of DMT and TMCD using 2D Heterogeneous Catalysts.....	27
3.4 Transesterification Product Characterizations	28
3.5 Additional Characterizations of 2D Heterogeneous Catalysts.....	34
3.6 Experiments for Leaching and Reusability of 2D Heterogeneous Catalysts	37
3.7 Experiments for Alternative Monomers	41
CHAPTER 4: Conclusions	43
REFERENCES	44
APPENDICES	49

LIST OF TABLES

Table 2.1	Reported comparison of various catalysts and their effect on the product [12].	5
Table 2.2	Comparison of percent FAME yields suggesting the reusability of heterogeneous catalysts in two different reported articles [25,26].	11
Table 2.3	Reported percent conversions and percent selectivities from transesterification reactions between DMT and EG using different catalysts [27].	13
Table 2.4	Reported comparison of percent FAME yield from various catalysts against GO-based separable heterogeneous catalyst [18].	16
Table 3.1	Elemental compositions of GO and GO-Sn based on XPS analysis.	24
Table 3.2	Elemental compositions of MX and MX-Sn based on XPS analysis.	24
Table 3.3	ICP-MS analyses of various samples to determine the amount of tin leaching (all samples are filtered unless stated otherwise).	32
Table 3.4	Percent DMT conversions of leaching experiment using three different solvents.	39
Table 3.5	Transesterification reactions between DMT and different diols using GO-Sn catalyst.	42

LIST OF FIGURES

Figure 2.1	Mechanism of transesterification reaction between DMT and TMCD.	5
Figure 2.2	Reported methanol yield from transesterification reactions between DMT and TMCD using various homogeneous metal catalysts [15].	6
Figure 2.3	Proposed mechanism of dibutyltin oxide during transesterification reaction.....	7
Figure 2.4	Different areas of petroleum processing that currently rely heavily on heterogeneous catalysts as indicated by the dotted arrows [7].	9
Figure 2.5	Structural schematics of graphene and MXene nanosheets [28,32].	15
Figure 3.1	Reaction schemes for preparing 2D heterogeneous catalysts.	19
Figure 3.2	DLS analyses of GO and MX nanosheets to determine the average thickness.	21
Figure 3.3	SEM images of GO (noted A and B) and MX (noted C and D) nanosheets to determine the average lateral size.	21
Figure 3.4	FTIR spectra comparison between GO and GO-Sn.....	22
Figure 3.5	XPS spectra comparison between GO and GO-Sn.	23
Figure 3.6	XPS spectra comparison between MX and MX-Sn.....	24
Figure 3.7	Proposed structure of GO-Sn catalyst.....	25
Figure 3.8	TGA analyses for GO/GO-Sn and MX/MX-Sn in air atmosphere.....	26
Figure 3.9	TGA analyses for GO, GO-Sn, MX, MX-Sn and Bu ₂ SnO in nitrogen atmosphere.....	26
Figure 3.10	Lab-scale setup for transesterification reaction.	28
Figure 3.11	Percent DMT conversions of transesterification reactions between DMT and TMCD using GO-Sn or MX-Sn catalyst at different tin loadings.	30

Figure 3.12	Percent DMT conversions of transesterification reactions between DMT and TMCD using GO-Sn catalyst (a) at different reaction temperatures and (b) from repetitive trials.....	30
Figure 3.13	Physical appearances of DMT/TMCD/GO-Sn oligomer products depending on the reaction temperature and time.	31
Figure 3.14	SEM images of GO and GO-Sn surfaces in various conditions.	35
Figure 3.15	EDX image of GO-Sn surface to determine the percent weight of tin.	36
Figure 3.16	Summarized workflow of filtration experiments.	37
Figure 3.17	Lab-scale setup for catalyst filtration.....	38
Figure 3.18	Percent DMT conversions of reusability experiment using three different solvents.....	40
Figure 3.19	Modified chemical structure of GO-Sn catalyst.	41

CHAPTER 1: Introduction

1.1 Backgrounds

In a chemical synthesis like transesterification reactions between a diester group and a diol group, typically a catalyst is used to expediate the process by changing the mechanisms of how the reaction happens, in which it lowers the overall activation energy required for the reaction to occur. While this allows for an energy efficient method of chemical synthesis, the use of a catalyst could also introduce other problems including visual change to the product, performance degradation, or environmental and health concerns if not properly deactivated or removed from the final product. The deactivation would be beneficial as long as residual catalysts do not cause any negative side-effects, but then the reusability is out of the picture. Then, it becomes a logical solution to entirely remove the catalyst from the product to avoid such issues and possibly reuse it in a different batch; however, efficient catalyst removal is a quite challenging process with a varying degree of success in a large-scale reaction. This is especially true for homogeneous catalysts as they are generally more difficult to remove from the reaction media when compared to that of heterogeneous catalysts [1,2,3].

1.2 Objectives

In light of this, the development of a heterogeneous catalyst capable of transesterification was brought to our attention as a collaborative and confidential project between Eastman Chemical Company and NC State Wilson College of Textiles. This new catalyst should exhibit reaction results that are comparable to currently available catalysts, while being able to eliminate undesirable metal catalysts from the final product. The target reactants for transesterification reactions are dimethyl terephthalate (DMT) and 2,2,4,4-tetramethyl-1,3-cyclobutanediol (TMCD), in which TMCD monomer is a key intermediate for novel products at Eastman Chemical

Company. Our work will focus on synthesizing a heterogeneous catalyst based on a two-dimensional matrix and demonstrate its efficient catalysis for the mentioned reactants and separability from the final products.

CHAPTER 2: Literature Review

2.1 Homogeneous Catalyst

In order to explore the possibilities of heterogeneous catalysts, a homogeneous one has to be understood first. A homogeneous catalyst is defined as a catalytic substance that becomes uniformly soluble in the composition and considered the same phase as that of the reactants. Homogeneous catalysts are highly recognized for their great efficiency without the need for extreme reaction conditions. This is possible while maintaining good selectivity and activity to the reactants even in low catalyst concentration [1]. Typically, these homogeneous catalysts include organometallic compounds, which are combined structures between an organic molecule and a metal from alkaline and transition metals, or sometimes other elements including but not limited to tin or boron [4]. Depending on their design and function, one can use a homogeneous catalyst to carry out hydrogenation, carbonylation, oxidation, or even polymerization reaction of various reactants to quickly and efficiently synthesize the final product [5,6]. In the earlier years of development, common polymers like polyethylene and polyester were made with simple transition metals. Both chromium and titanium were proving to be very effective in large-scale industrial settings, while more complex catalytic compounds began to emerge like soluble titanium- or aluminum-based catalysts called Ziegler-Natta. Catalysts like these are very effective for various polymerization syntheses while benefiting from enhanced product properties and lower manufacturing costs, and there are on-going efforts to incorporate catalytic metals to different organic compounds to develop highly selective and highly active catalysts [7].

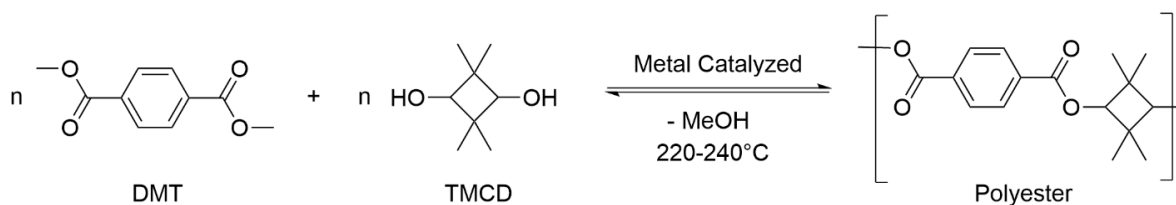
While homogeneous catalysts are extensively used in various chemical processes, they are not without their other shortcomings. First, the area where the homogeneous catalysts become disadvantaged when compared to the heterogeneous one is the complications of separating it from

the reaction medium. Generally, the removal or deactivation of catalysts involve complex processing and resources, not to mention the huge amount of waste it produces that raise environmental concerns. On the other hand, if left untreated, it would become the culprit of defects in the final product such as color change, properties change, and performance degradation. Then, there also is the problem of corrosion deposits building up in large-scale industrial reactors and potentially causing undesirable effect to the manufacturing process [8,9].

As for the choice of a catalytic metal to use in our transesterification reaction and further develop into a heterogeneous catalyst, the literature shows that tin has proven to be the most commonly used and efficient catalyst [10,11]. A paper by Pang et al. reviews a novel chemical process of making polyesters via ring-opening mechanism, which includes the transesterification reaction as one of the key steps to prepare cyclic oligomer precursors for the follow-up reactions [8]. For this transesterification step, dibutyltin oxide was the most commonly picked catalyst besides zinc acetate and few others, while being capable of producing high molecular weight polyesters with great efficiency. Notably, one of the mentioned articles demonstrates how organotin catalysts exhibit better performance in efficient monomer conversions when compared to the other types, while having little to no defects like undesirable color changes in the final product [12]. Table 2.1 summarizes the reaction results based on the equal amount of catalyst concentration at the same temperature. Both dibutyltin dichloride and 1,3-dichloro-1,1,3,3-tetrabutyl distannoxane are organotin catalysts; and while dibutyltin dichloride is capable of producing high molecular weight polyester at only 64% conversion, 1,3-dichloro-1,1,3,3-tetrabutyl distannoxane is able to yield 91% in just 20 minutes of reaction runtime. Overall, organotin-based catalysts show great potential according to the literature and were deemed viable for the transesterification reaction needed for this research.

Table 2.1 Reported comparison of various catalysts and their effect on the product [12].

Catalyst	Conc. (mol %)	Temp (°C)	Time (min)	Conv. (%)	M _w (g/mol)	Product Color
None	0	222	480	34	11,000	Yellow
4-dimethyl-aminopyridine	0.4	222	240	26	14,000	Colorless
Stearic acid/lithium salt	0.4	222	120	14	4,800	Yellow
Cyclohexyltriphenylphosphonium tetraphenylborate	0.4	222	180	98	36,000	Yellow
Dibutyltin dichloride	0.4	222	240	64	44,500	Colorless
1,3-dichloro-1,1,3,3-tetrabutyl distannoxane	0.4	222	20	91	24,800	Colorless

**Figure 2.1** Mechanism of transesterification reaction between DMT and TMCD.

Particular to our interest in performing transesterification reaction between dimethyl terephthalate (DMT) and 2,2,4,4-tetramethyl-1,3-cyclobutanediol (TMCD) as illustrated in Figure 2.1, only a few patents specifically discuss it and one of them notes that polyesters from these two can be synthesized by different types of homogeneous metal catalysts with varying degrees of success [13,14]. A study of catalytic activities of various metals including cobalt ($\text{Co}(\text{OAc})_2$), zinc ($\text{Zn}(\text{OAc})_2$), manganese ($\text{Mn}(\text{OAc})_2$), titanium ($\text{Ti}(\text{OBu}_2)_4$), sodium (NaOAc), germanium ($\text{Ge}(\text{OEt})_4$), antimony (Sb_2O_3), and most importantly tin (Bu_2SnO) have been investigated with DMT and TMCD at reaction temperature of 240 °C over the course of couple hours. The results from the report are illustrated in Figure 2.2, and they estimate the extent of activity based on the

amount of methanol by-product yield. While half of the tested catalysts only produced trace amounts of methanol, the other four produced notable percent yields while dibutyltin oxide (Bu_2SnO) was highest under the same circumstances [15]. Theoretically, the approximate result of 80% methanol yield would mean 80% conversion of DMT monomers into the final product. Here, the percent conversion between DMT and TMCD may not be as high as that of between DMT and some other primary diols like ethylene glycol (EG) because TMCD has secondary alcohol structures which would be more stable and less reactive compared to that of a primary alcohol. Furthermore, the nucleophilic oxygen of TMCD is also sterically hindered by neighboring methyl groups which may contribute to the difficulty attacking the electrophilic carbonyl carbon. Despite the lower than expected percent conversions of DMT and TMCD observed in the literature, even more typical catalysts, namely titanium alkoxides, were found to be less effective than dibutyltin oxide, which has shown the most promising result out of many other organometallic catalysts [15].

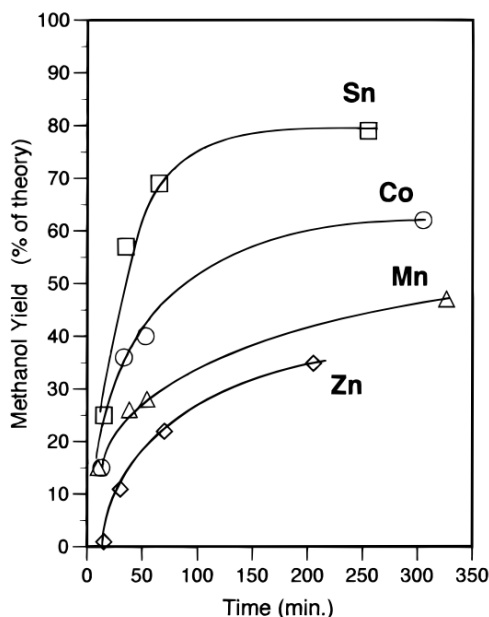


Figure 2.2 Reported methanol yield from transesterification reactions between DMT and TMCD using various homogeneous metal catalysts [15].

The reaction mechanisms of homogeneous catalysts are generally well studied and documented in the literature. This is also true for tin-based organometallic catalysts used in transesterification synthesis. The working mechanism of organotin catalysts can be distinguished into two major types: Lewis acid method or exchange/insertion method. The former is much more common way for transesterifications and also appropriate for how dibutyltin oxide would behave. This is because dibutyltin oxide does not have an exchangeable group to transfer to and from the alcohol reactant. Therefore, based on the Lewis acid method, the tin compound behaves like a Lewis acid and coordinates itself with the carbonyl oxygen of the ester reactant. This then polarizes the carbonyl carbon and increases the chance of being attacked by a nucleophilic oxygen of a hydroxyl end-group. Meanwhile, the hydroxyl group of alcohol reactant may also be coordinated with the tin compound via hydrogen bonding, which would keep both reactants in close proximity for the nucleophilic attack to happen. This would explain the increased reaction rate between the two reactants. Finally, the leaving alkoxide ion from the ester abstracts the hydrogen to form the alcohol by-product. From this information, the proposed mechanism of dibutyltin oxide for our transesterification reaction is illustrated in Figure 2.3 [16,17,18].

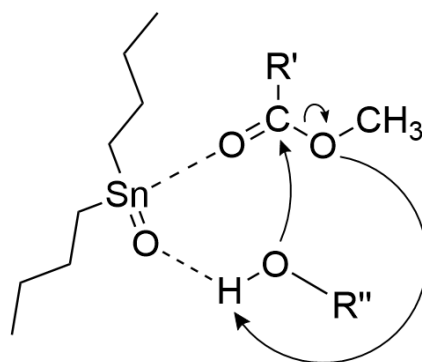


Figure 2.3 Proposed mechanism of dibutyltin oxide during transesterification reaction.

2.2 Heterogeneous Catalyst

On the contrary to a homogeneous one, a heterogeneous catalyst is defined as a catalytic substance that is immiscible and its phase remains different from that of the reaction medium. Because of this insoluble nature, the main advantage of heterogeneous catalysts is that they are not consumed during the reaction, therefore they could possibly be reused in a different batch for another run of catalysis. Especially for large-scale reactions operating in most of chemical industries, this undoubtedly becomes a very valuable element as it lowers the manufacturing cost while saving resources at the same time. The basic fundamentals are similar to those of homogeneous ones as it is usually the metal species that catalyze the reaction, but this time, an insoluble solid support is the essential component required to keep the metal anchored as a part of the catalyst. It is this solid support that grants the heterogeneous quality because it does not become uniform in composition with the mixture, as a result, the phase separation by filtration or decantation can be used to recover and recycle these catalysts again [9,19]. Also, this potentially eliminates the undesirable effects on the final product like color change or performance degradation. Furthermore, they are typically more thermally stable and can be used in wider scope of reactions than that of the homogeneous catalysts. While homogeneous catalysts have a relatively shorter life cycle and have to be converted back to active state again, the heterogeneous catalysts are less prone to deactivation and could last for several runs [7,9]. Due to these reasons, the heterogeneous catalyst is much more favorable when it comes to industrial processes, accounting for roughly 90% by volume in chemical production [20]. A few examples where heterogeneous catalysis is heavily practiced include oxidation reactions, ammonia synthesis, and many areas of petroleum processing as shown in Figure 2.4 [7].

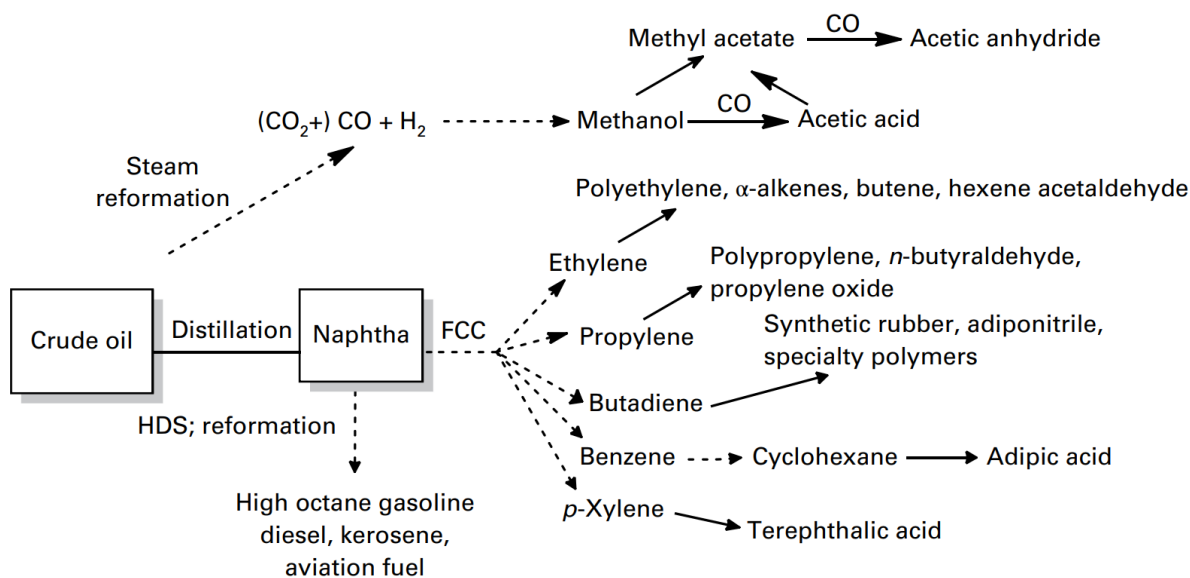


Figure 2.4 Different areas of petroleum processing that currently rely heavily on heterogeneous catalysts as indicated by the dotted arrows [7].

However, there are some drawbacks to these heterogeneous catalysts as well. In the literature today, there are far fewer publications discussing the mechanism of how these catalysts work. This is because the catalytic performance is mainly analyzed and understood at a molecular level, while having a solid supporting mass renders it much more complex to characterize via current spectroscopic methods. Therefore, for the heterogeneous catalysts, it becomes reasonable to derive the working mechanisms from a similar homogeneous catalytic system as they are well-documented and less ambiguous. Another area that a homogeneous one would outperform a heterogeneous one is the level of selectivity and activity. The whole homogeneous catalyst serves as one active site that triggers the reaction, whereas a heterogeneous catalyst may possess different types of active sites that are spread throughout the surface of a solid structure. Not only does this contribute to lower degree of selectivity, but also the activity of these catalysts is hindered by lower mass transfer, or the extent of diffusion, throughout the reaction medium [4,7]. The behavior of a heterogeneous catalyst can be explained by the Langmuir-Hinshelwood effect, which models the

interaction of two molecules based on adsorption/desorption reactions. It can only catalyze a chemical reaction when the adsorption takes place, which refers to a reactant getting coordinated to the metal located on the solid's surface. Just like how a typical enzyme would work, this active site allows for the reaction to occur and finally desorbs, or dissociates, the reactant back out from the catalyst [20].

The use of heterogeneous catalysts for a transesterification reaction is nothing new. As of today, the research and development are heavily focused on the biodiesel production that uses transesterification to convert triglyceride and alcohol into fatty ester and glycerol. The relatively recent surge of interest in producing usable fuels from renewable resources including vegetable oils or animal fats have pursued after these heterogeneous catalysts for both environmental and cost reasons. Although this is not a polycondensation reaction like that of DMT and TMCD, they are fundamentally the same transesterification reaction and there are few key points that could be learned from the literature. Generally, a heterogeneous catalyst for these reactions requires higher temperature and pressure to achieve the comparable degree of conversion as that of a homogeneous catalyst because the mass transfer is restricted by the introduction of solids into the system [21,22]. In this case, the low mass transfer could somewhat be alleviated by forcing vigorous agitation using an ultrasonication, because it is able to increase the reaction rate by having catalytic solids well dispersed into the reaction mixture [23,24]. Additionally, the reusability and leaching of metal catalysts are very important aspects to note from the literature. One article reports that a zinc-doped calcium oxide (Zn/CaO) catalyst is able to run five successive cycles of reaction with over 99% product yield after being recovered from the mixture via simple filtration and reactivating it. However, a gradual decrease in catalytic performance was observed for the last two runs and this could be from either an unknown structural change during the regeneration step or a partial

leaching of the active metal species from the solid support [25]. Another article reporting of decomposed dolomite (CaO and MgO) as a heterogeneous catalyst shows close to ~92% product yield for the first three runs, followed by a slight loss of catalytic activity in the fourth run. It is not until the catalyst is regenerated for the fifth run that showed a slight better performance than one before. The culprit may be that CaO is soluble in methanol and possibly leached the active site after certain amount of usage [26]. The said reaction yields are shown in Table 2.2. Out of the two, the former study on Zn/CaO also tested for the leaching of metals from the heterogeneous catalyst. After a test run using 5 wt% Zn/CaO (50000 ppm) followed by a filtration, it was found that very small amounts of Ca²⁺ (5 ppm) and Zn²⁺ (8 ppm) metal ions were detected from the FAME product samples using atomic absorption spectroscopy. To further explore on this idea, the Zn/CaO heterogeneous catalyst was vigorously washed with methanol and filtered out. The obtained methanol was used as the reactant to run a follow-up transesterification reaction, which yielded about 5% FAME product [25]. From this, it is important to note a small amount of leaching may occur at some point during the reaction, depending on the interaction strength between the metal and solid support. The leached metal ions are then able to catalyze the reaction behaving like an ordinary homogeneous catalyst; however, the insignificant amount of conversion suggests that filtering the heterogeneous catalysts does remove majority of the metal species from the product.

Table 2.2 Comparison of percent FAME yields suggesting the reusability of heterogeneous catalysts in two different reported articles [25,26].

Article	Fatty Acid Methyl Ester (FAME) Yield (%)						
	Run 1	Run 2	Run 3	Run 4	Run 5	Run 6	Run 7
Kumar et al.	>99	>99	>99	>99	>99	~68	~36
Ilgen, O.	~91	~92	~91	~75	~82		

Specifically for a transesterification between DMT and diol reactants, it can be carried out as an acid- or a base-catalyzed reaction. Due to the Lewis acid behavior of dibutyltin oxide catalyst, it is safe to assume a heterogenized dibutyl oxide would undergo an acid catalysis. However, the polymer-side of heterogeneous catalyst application is almost non-existent in the literature, instead many transesterification syntheses discuss the use of homogeneous catalysts and this is especially true for acid catalyzed polycondensation reactions. Being the closest to our objective, one article by Meyer et al. uses heterogeneous basic catalysts based on zeolite solid to conduct transesterification reactions between a DMT and ethylene glycol (EG) [27]. The zeolite powder was ion-exchanged with sodium and cesium to prepare two different catalysts, which were then calcined to remove any water and carbon dioxide content. As a result, the two zeolite catalysts exhibit the basic property that is required for base catalyzed reaction. The percent DMT monomer conversions using these catalysts at 180 °C for 6 hours are presented in Table 2.3. Although there isn't a comparable control using a homogeneous catalyst, the data reveals that zeolite solids are very capable of high catalytic activity in terms of DMT conversion with the added benefit of easy separation from the reaction medium. The more interesting aspect to note from this study is the level of selectivity of these catalysts to the desired product. The transesterification between DMT and EG is a polycondensation reaction because there is a bi-functional end-group on each end of these monomers. In small lab-scale reactions, the possible product formation includes two different oligomers: 2-hydroxyethyl terephthalate (HET) or bis(2-hydroxyethyl) terephthalate (BHET). The desired product is BHET, which both end-groups of DMT have condensed to form a trimer structure; whereas HET is a less desirable product where only one side has reacted to form a dimer. Here in this case, the stronger basic catalyst Cs₂O/CsX has outperformed the weaker basic NaX in the selectivity towards BHET [27]. It is important to consider that the level of acidity or basicity

would affect the selectivity of the final product. In other words, the formation of a desired product between DMT and TMCD using dibutyltin oxide may also depend on the strength of coordination between the tin species and the carbonyl oxygen. Besides this particular study, there is seemingly no other literature that discuss what we seek to achieve, which makes it a considerably more lucrative subject to investigate. As per Eastman’s remark, there is still no commercially available heterogeneous catalyst designed to be separable from the polymeric product synthesized in an industrial-scale transesterification reaction.

Table 2.3 Reported percent conversions and percent selectivities from transesterification reactions between DMT and EG using different catalysts [27].

Catalyst	Loading Conc. (mol DMT/g cat.)	DMT:EG (molar ratio)	DMT Conv. (%)	Selectivity to HET (%)	Selectivity to BHET (%)
None	None	1:5	22	100	0
NaX	1	1:5	95	100	0
Cs ₂ O/CsX	1	1:5	94	28.7	58.5

2.3 Two-Dimensional Matrix Catalyst

Currently in the Wilson College of Textiles, especially with Dr. Gao’s research focus, a material like graphene is of high interest for various practical applications given their unique features. Then naturally, a graphene sheet becomes an appealing subject to explore for its potential as a solid base of the heterogeneous catalyst. In a similar manner, MXene—pronounced as maxene—became a noteworthy material to be investigated as a solid support as well. Graphene is a single-atom thick, two-dimensional layer composed of carbon atoms arranged in a form of hexagonal lattice as shown in Figure 2.5a [28]. Despite its extreme thinness ranging from 0.35 nm to 1.00 nm, graphene is one of the strongest materials that can withstand forces up to 200 times greater than a steel of the same mass, while also exhibiting outstanding electrical and thermal

conductivities that allow for versatile uses [29]. This is because each carbon atom in a graphene layer is connected to three other carbons by sigma-bonds (sp^2) and an electron can hop over the whole planar structure through conduction and valence bands [30]. However due to its very high specific surface area, graphene tends to form agglomerates that get stuck together via Van der Waals and π - π interactions. This problem can be avoided by attaching other molecules to the surfaces of graphene nanosheet, which in turn introduces bulk-sized moieties that can disrupt the intermolecular interactions. Moreover, it would promote the dispersion of said graphene sheets depending on the hydrophilic or hydrophobic nature of attached molecules and the media [29]. On the other hand, MXene is also a two-dimensional sheet consisting of transition metal carbides with a chemical formula of $M_{n+1}X_nT_x$ where T refers to a termination group such as oxygen or hydroxyl on the surface of nanolayer [31]. Unlike graphenes, MXenes are typically multi-layered structures with titanium and carbon atoms sandwiched together along with numerous oxygen groups on the surface as illustrated in Figure 2.5b [32]. Also, due to the lack of any functional group on the graphene sheet, it may be necessary to oxidize the graphene layer to make a graphene oxide, which introduces potential active sites for the metal species attachment. To achieve this, the Hummer's method is typically used to synthesize oxidized graphene sheet from powdered graphite flakes, providing a oxygenated surface features in which the catalytic moieties can tether [33]. As for the characteristics of MXenes, they are highly capable in electrical conductivity as compared to graphenes; however, they also experience the similar agglomeration issue as mentioned previously [34]. While the presence of surface terminal groups would allow MXenes to be easily dispersed in an aqueous solution, taking the similar approach of grafting other larger molecules to the surface of these nanosheets would further help the dispersion required for catalytic reactions.

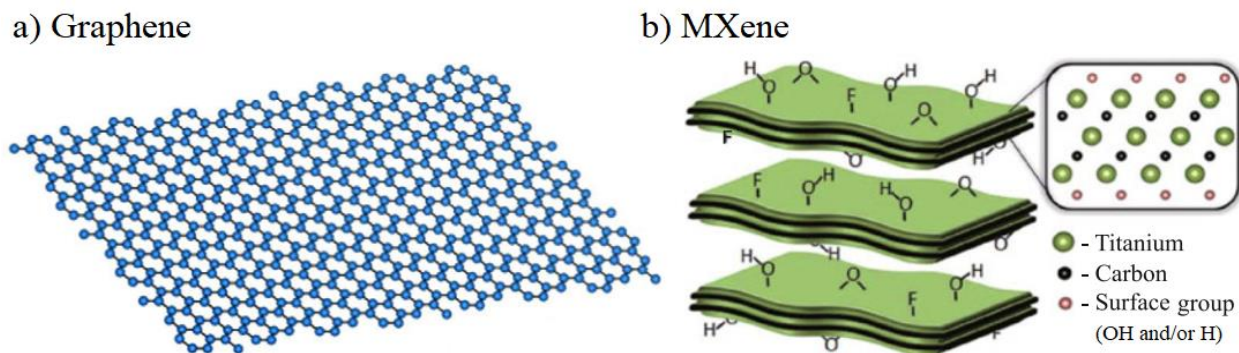


Figure 2.5 Structural schematics of graphene and MXene nanosheets [28,32].

The use of graphene or graphene oxide (GO) as a functional heterogeneous catalyst for biodiesel production has been reported few times in the literature. The majority of these articles prepare their GO-catalysts by first using the modified Hummer's method to synthesize GO solids [33], and using *in situ* impregnation to graft catalytic species onto the surface of the GO material. Depending on the modification used for the Hummer's method, it typically produces GO flakes that are as small as 5 μm to as large as 100 μm in lateral size with the surface area ranging anywhere from 50 μm^2 to 7000 μm^2 [35]. These flakes are able to exfoliate and disperse into individual layers in an aqueous solvent by the help of partially charged chemical moieties, which provides much larger surface area needed for chemical reactions. Given that, the impregnation method generally involves long period mixing of GO suspension with the desired catalytic species under heat, followed by rinsing, drying, and calcinating them to obtain GO-catalysts with secure attachment of catalytic species [18,36,37]. As for the actual catalytic experiment, the GO-catalysts are re-dispersed in solvents like methanol to run the reaction, and separated from the reaction medium using a simple filtration method [37]. For example, Ali et al. studied GO-based NaOH-bentonite catalyst for biodiesel transesterification reactions. The comparison between this catalyst and few others reported in the article is shown in Table 2.4 [18]. In this case, the data suggests that GO-NaOH-bentonite is very efficient and competent when compared to other homogeneous catalysts

in terms of catalytic activity, even in relatively mild reaction conditions. While the outcomes of catalysis look promising, the vital feature of this 2D matrix-based heterogeneous catalyst is an efficient removal of active catalytic moieties from the product, so that any potential defects would be eliminated from the final product. Despite the study informing the gradual loss of catalytic performance from ~98% to ~10% FAME yield over the course of five transesterification reactions, there is a positive note that the leaching of active species from GO matrix was not observed. However, this remains questionable as the leaching experiment was conducted with GO-catalyst being stirred only in methanol at 110°C for 2 hours, then filtered so that the methanol filtrate was used as the reactant to observe any conversion to FAME product. While this may eliminate heat and agitation from the picture, it does not dismiss the possibility of catalytic species detaching during the process of actual catalytic interactions with ester and alcohol molecules. Unfortunately, there are no other leaching tests reported in the literature to approach this concern in a different manner, so it may be worthwhile to investigate using a recovered catalyst from the first run of catalysis to test for any leaching.

Table 2.4 Reported comparison of percent FAME yield from various catalysts against GO-based separable heterogeneous catalyst [18].

Catalyst	Time (hr)	Temp. (°C)	Loading (wt%)	Alcohol:Oil (molar ratio)	FAME yield (%)
GO-NaOH-bentonite	4.5	62	6	6:1	98.5
Bi ₂ O ₃ -La ₂ O ₃	4	150	2	15:1	93
La ₂ O ₃ -ZnO	3	60	5	6:1	30
W-CaO/hydroxyapatite	7	120	8	6:1	99

CHAPTER 3: Experiments and Discussion

3.1 Synthesis of 2D Heterogeneous Catalysts

The synthesis of a new heterogeneous catalyst macromolecule involves two major wet-chemical processes: making of two-dimensional (2D) matrices such as graphene oxide (GO) or MXene (MX) that will serve as the substrate, and grafting of commercially available catalyst dibutyltin oxide ($\text{Sn}(\text{Bu})_2\text{O}$ or $(\text{C}_4\text{H}_9)_2\text{SnO}$) onto that matrix surface via chemical means. The required reagents for the experiment including graphite powder, Ti_3AlC_2 powder, sulfuric acid, nitric acid, hydrogen peroxide, hydrochloric acid, potassium permanganate, lithium fluoride, dibutyl oxide, butylamine, toluene, and various other solvents were commercially purchased in chemical grades.

First of all, large-sized GO nanosheet samples were prepared using Hummer's method with few modifications [33,38]. A mixture of 150 mL concentrated sulfuric acid (>98%) and 50 mL nitric acid (~68%) were mixed with 3 g of graphite powder for 12 hours. Then, the mixture was diluted in 1 L of water, filtered through a filtration paper with some additional rinse, and dried at room temperature for 24 hours. This graphite was heated by microwave irradiation at 750 watts for 90 seconds to obtain expanded graphite powder. This expanded graphite was added to 400 mL of concentrated sulfuric acid to be stirred for 1 hour, followed by slow addition of 18 g of potassium permanganate. This reaction process was cooled under 0 °C with silicon oil and kept stirred for an additional hour. Then, it was heated to 50 °C for 12 hours and cooled to obtain oxidized graphite mixture. After pouring the mixture into 1 L of ice water, drops of 30 % hydrogen peroxide were added to stop the oxidation process until steady bright yellow is observed and set for 4 hours. The supernatant was dumped and the remainder was repetitively rinsed with 1 M hydrochloric acid solution and plenty of deionized water to remove residual metal and acid until

pH close to 5 was achieved. Finally, centrifugation and repeated rinsing with water yields thickened GO gel, which is then vacuum-filtered and dried at room temperature for at least 72 hours to form a thick black film.

On the other hand, large-sized MX nanosheet samples were also made according to the MILD method reported in literature [39]. First, 4.8 g of lithium fluoride was added to 60 mL of 9 M hydrochloric acid and stirred for 5 minutes to prepare an etchant solution. Soon after, 3 g of Ti_3AlC_2 powder was slowly added over the course of 5 minutes and set for 24 hours at room temperature for the reaction to run. The acidic mixture was then washed with deionized water using several cycles of centrifugation at 3500 RPM for 5 minutes each, which resulted in acidic supernatant that needs to be decanted before adding more deionized water for the next cycle. The rinsing process was repeated and observed for acidity until neutral pH close to 5 was achieved. It would generally take roughly three cycles when using a 175 mL centrifuge tube or eight cycles when using a 50 mL centrifuge tube. When sediments settled at the bottom and a dark-green supernatant was observed, the black layer of $\text{Ti}_3\text{C}_2\text{T}_x$ slurry on top of nonetched $\text{Ti}_3\text{AlC}_2/\text{Ti}_3\text{C}_2\text{T}_x$ mixture was carefully separated and collected for the final step. The slurry is then vacuum-filtered and dried at room temperature for at least 72 hours to form a thick black film.

The reaction setup for grafting a commercial catalyst, dibutyltin oxide, onto both 2D matrices made above involved a three-neck round bottom 250 mL flask placed on a lower hemispherical heating mantle, along with a Graham condenser on the middle neck sealed with some grease. A temperature probe linked to J-KEM Scientific 260 instrument was inserted into one of necks and sealed with Teflon tape. Then, 0.8 g of 2D substrate, either of GO or MX, was dispersed into the flask filled with a solution of 40 mL dry toluene (2%) and 4 mL butylamine. Here, butylamine was introduced to deprotonate the hydroxyl groups while exfoliating the 2D

nanosheets. Preferably, the large-size films of 2D samples were carefully broken into smaller flakes using forceps to help further with the dispersion. The vessel was then flushed with nitrogen gas and heated at 60 °C for an hour while being stirred with a magnetic stir bar. The mixture was allowed to cool and kept stirred for 24 hours, and a nitrogen gas filled balloon was injected through the rubber septum to continuously purge the reaction vessel. Next, 0.656 g of dibutyltin oxide was carefully added to the flask and the whole setup is completely sealed for a dry reaction. Then, the mixture was stirred and heated at 110 °C for additional 24 hours. Once the reaction mixture cooled down to room temperature, a bit of acetone was added to help it pour through a vacuum filtration setup with Omnipore™ 0.1 µm hydrophilic PTFE filter paper. Three cycles of 100 mL of acetone were used to rinse the catalyst and left for 48 hours to completely dry on the filter paper in the vacuum setup. At this point, a similar looking, yet less glossy and more brittle black film was observed. This tin-grafted 2D catalyst sample was carefully peeled off from the filter paper and stored in a glass vial. The overall reaction scheme with images of the precursors and catalysts are shown in Figure 3.1.

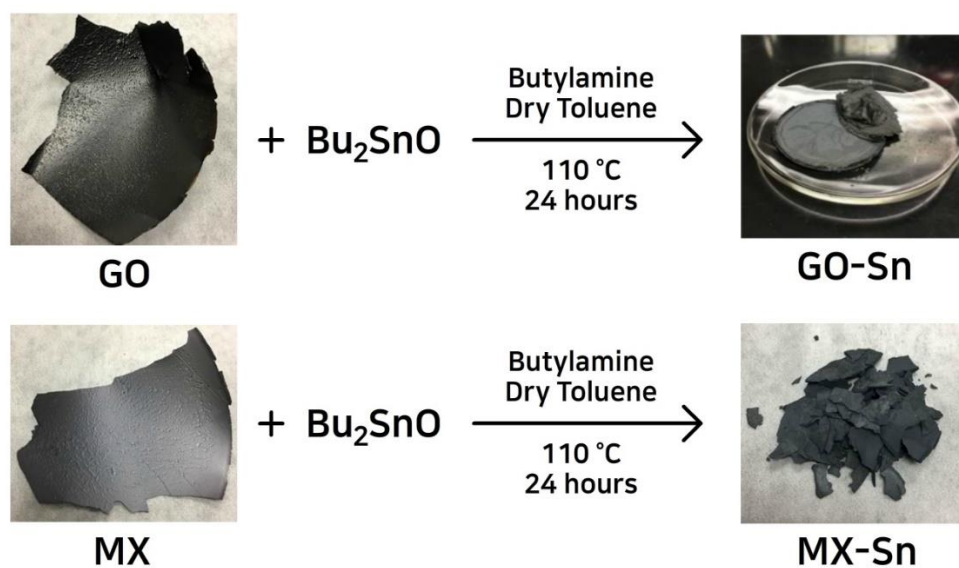


Figure 3.1 Reaction schemes for preparing 2D heterogeneous catalysts.

3.2 Preliminary Characterizations of 2D Heterogeneous Catalysts

Before moving forward with the transesterification reaction with our new catalysts, Dr. Shradha Patil—postdoctoral researcher who initially investigated on this project—examined the morphological and structural aspects of the catalysts using various methods including Dynamic Light Scattering Analysis (DLS), Scanning Electron Microscopy (SEM), Fourier-Transform Infrared Spectroscopy (FTIR), X-ray Photoelectron Spectroscopy (XPS), and Thermogravimetric Analysis (TGA).

First, DLS analysis was used to measure the Z-dimension or the depth of GO and MX flakes. The average of three sample submissions show 2.07 μm for GO and 3.32 μm for MX as shown in Figure 3.2. While DLS may be useful for spherical particles suspended in the liquid, it does not account for the rotations of 2D flakes. Plus, all the larger particles settled on the bottom and only the smaller particles were seemingly measured. The results may represent the thickness of small-sized flat particles, but do not accurately portray the actual size of them. For this reason, SEM analysis was also used to measure the lateral dimensions of GO and MX flakes. Figure 3.3 shows the images of 2D flakes widely varying in size. The average lateral sizes were measured to be roughly 35-50 μm for GO sheets and 5-8 μm for MX sheets.

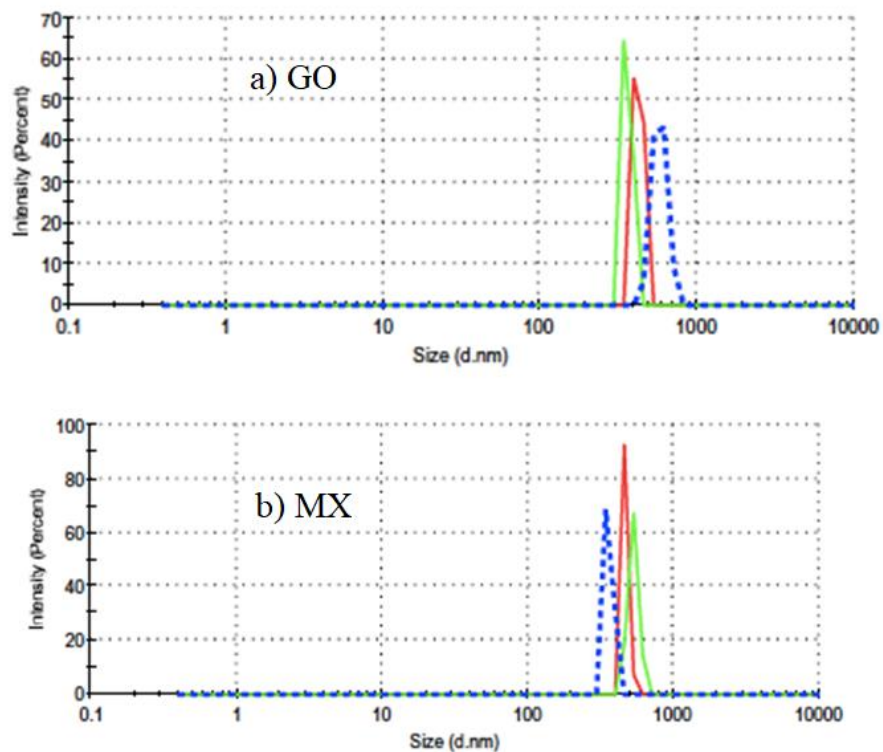


Figure 3.2 DLS analyses of GO and MX nanosheets to determine the average thickness.

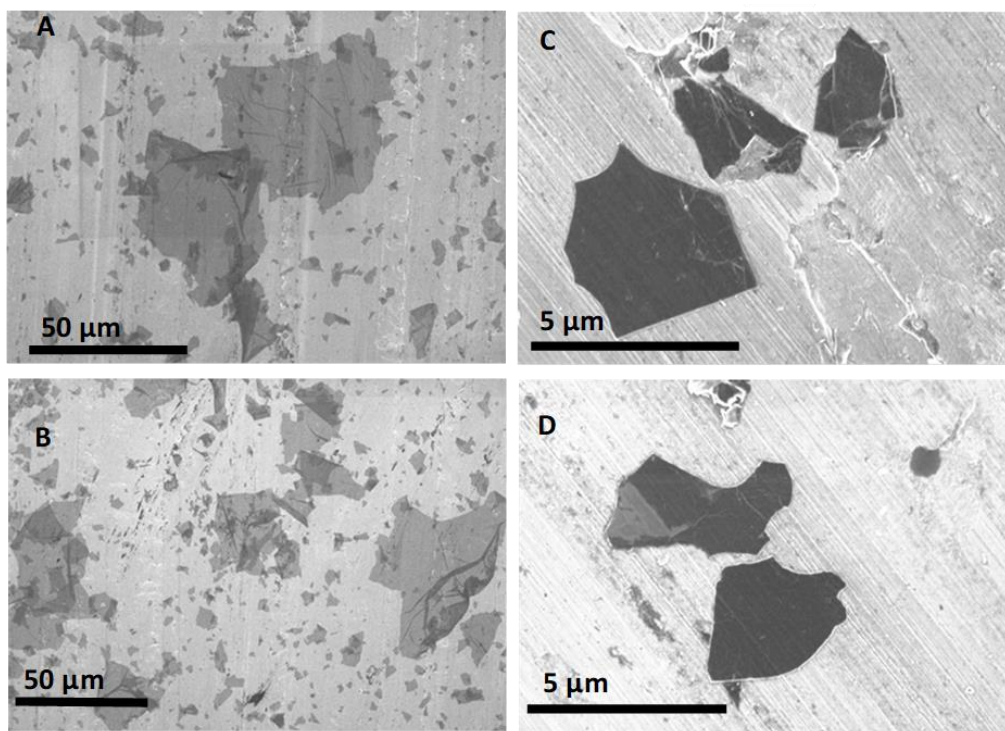


Figure 3.3 SEM images of GO (noted A and B) and MX (noted C and D) nanosheets to determine the average lateral size.

FTIR was used to study both the pristine GO sheet and the new GO/dibutyltin oxide catalyst (shortened as GO-Sn for ongoing discussion) for any changes in their functional groups. As shown in Figure 3.4, the spectra of GO and GO-Sn showed noticeable differences especially in 3300-3400 cm^{-1} region. Here, the broad curve typically suggests a hydroxyl (-O-H) stretching frequency which may be exhibited by oxidized graphene sheets that possess abundant hydroxyl groups. Whereas the other peak at 1000-1100 cm^{-1} region may be originating from epoxy (-C-O-C-) groups embedded in GO surfaces. The peaks and broad bands are observed for GO because it is a hygroscopic material that tends to absorb water. The suppressed signals observed in GO-Sn suggest oxygenated functional groups decomposing into by-products like H_2O and CO_2 upon heat exposure during the catalyst synthesis. The suppression of the signal does not necessarily mean the oxygenated functional features are replaced by tin compound, so an alternative characterization method is used to study the successful grafting of catalytic tin moiety.

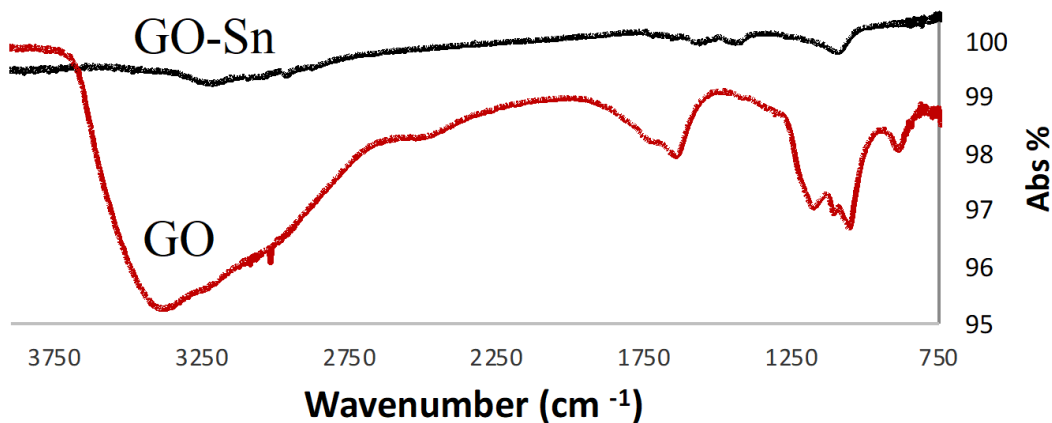


Figure 3.4 FTIR spectra comparison between GO and GO-Sn.

XPS was used to examine the surfaces of the GO-Sn and MX-Sn samples for the presence of elemental tin. Shown in Figure 3.5, the spectrum of pristine GO sheet showed that its surface only consisted of carbon and oxygen atoms, whereas the analysis of GO-Sn surface also detected elemental tin in addition to those two atoms. This suggests that dibutyltin oxide had been

successfully grafted onto the GO matrix. The elemental composition data in Table 3.1 reveals the level of oxidation in GO and presence of tin on its surface. From the introduction of dibutyltin oxide, the overall level of oxygen composition has significantly dropped from 37.4% to 13.8%, while the detection of 8.2% tin element on GO-Sn sample confirms the attachment of catalytic species to the surface. Interestingly, 1.7% of nitrogen was also present in the GO-Sn sample and it may have come from the butylamine reagent used as an exfoliator of GO during the grafting reaction. As for MX and MX-Sn, Figure 3.6 and Table 3.2 reveal that the usual carbon, oxygen, and titanium atoms are detected on the surface of pristine MX surface. In addition to these, the presence of chlorine and fluorine were also observed and they could be traced back to the synthesis of 2D MX sheets using lithium fluoride and hydrochloric acid to prepare hydrogen fluoride etchant solution. Otherwise, MX-Sn confirmed the detection of 7.6% tin element along with decreased atomic percentage of oxygen. However, there was no trace of nitrogen, which suggests butylamine was not present on the MX-Sn sample unlike that of GO-Sn. Based on this information, a schematic depicting the chemical structure of our new tin-grafted catalyst can be illustrated as shown in Figure 3.7, where the protruding hydroxyl groups present on the precursor GO sheets are replaced by the tin compounds.

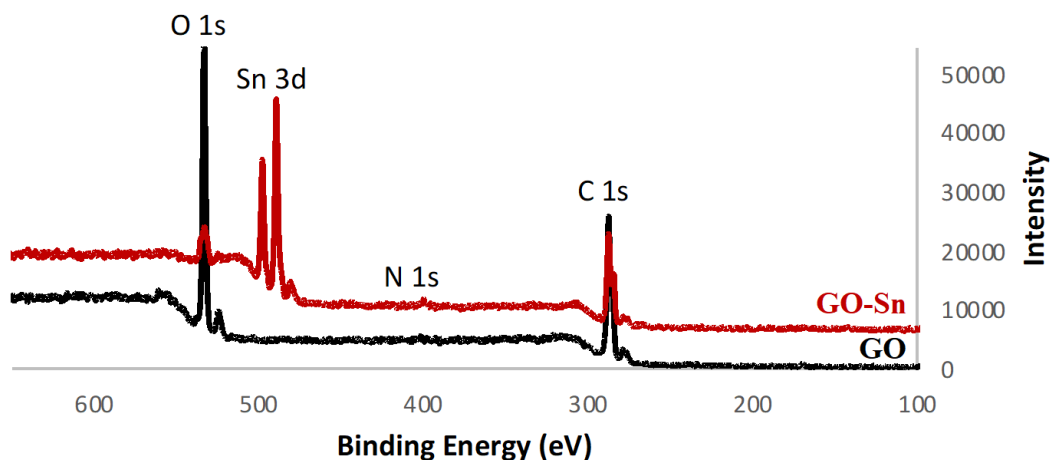


Figure 3.5 XPS spectra comparison between GO and GO-Sn.

Table 3.1 Elemental compositions of GO and GO-Sn based on XPS analysis.

Element	GO (atomic wt%)	GO-Sn (atomic wt%)
Carbon	62.6	76.2
Oxygen	37.4	13.8
Tin	-	8.2
Nitrogen	-	1.7

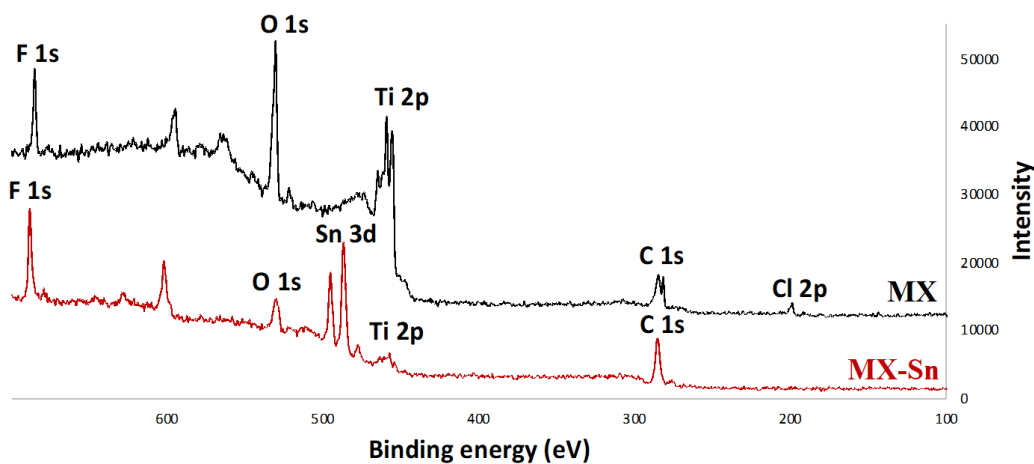


Figure 3.6 XPS spectra comparison between MX and MX-Sn.

Table 3.2 Elemental compositions of MX and MX-Sn based on XPS analysis.

Element	MX (atomic wt%)	MX-Sn (atomic wt%)
Carbon	30.6	50.6
Oxygen	34.8	16.3
Titanium	23.1	3.6
Fluorine	9.2	21.9
Chlorine	2.4	-
Tin	-	7.6

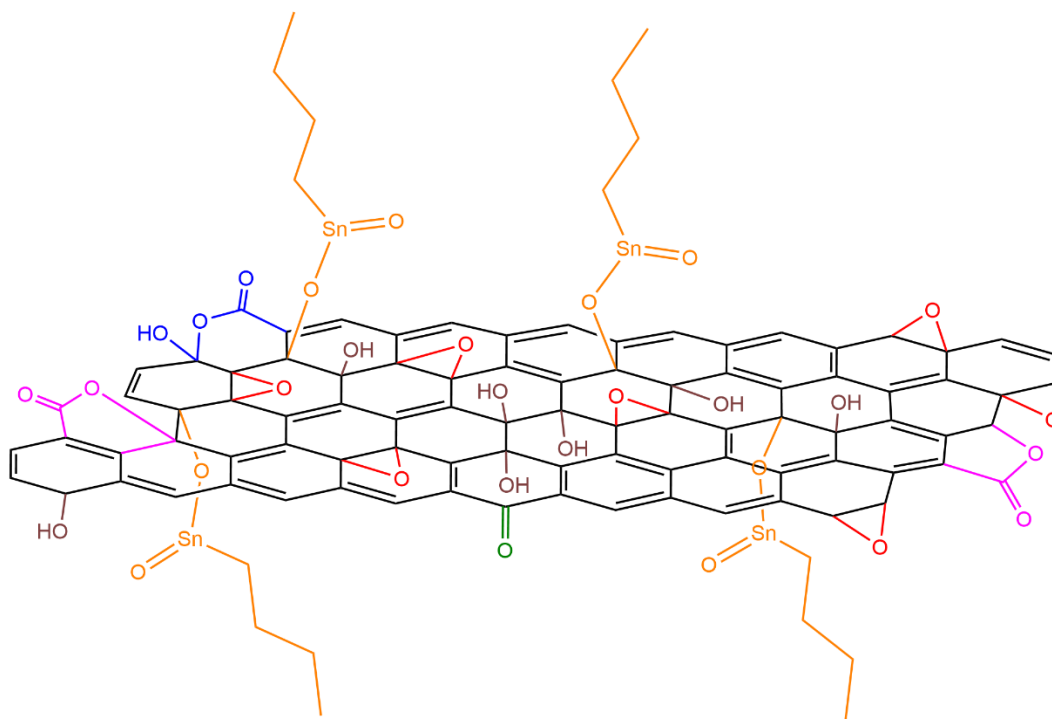


Figure 3.7 Proposed structure of GO-Sn catalyst.

TGA was used to better understand the composition and thermal properties of our new catalysts. The ramping rate was set to 2 °C/min and heated up to 800 °C in air atmosphere. According to Figure 3.8a, there is 42.46 wt% mass difference between GO and GO-Sn samples at the final temperature. If this difference is assigned to the oxidation product SnO₂, the elemental tin composition would be calculated to be 33.4 wt% of the GO-Sn catalyst. The GO curve dropping to zero at such high temperature also suggests that everything would decompose in air except for the tin oxide component. The similar approach for MX shown in Figure 3.8b suggests that elemental tin is 67.8 wt% of the MX-Sn catalyst. Unlike that of GO and GO-Sn, the MX-Sn has lost more mass compared to that of MX due to the presence of titanium atoms and the loss of butyl groups from tin component that accounted for higher overall carbon composition. As for decomposition in nitrogen atmosphere (Figure 3.9), both GO-Sn and MX-Sn catalysts seem to withstand temperatures up to 230-240 °C without major weight loss. Although slightly concerning,

Eastman has noted transesterification reaction between DMT and TMCD is expected to happen around 227 °C and the thermal stability of the catalysts is just enough to deliver the desired result by a small margin. According to these preliminary tests, the previously mentioned two values of 33.4 wt% for GO-Sn and 67.8 wt% for MX-Sn will be used to calculate the concentration of elemental tin loading needed for the future reactions.

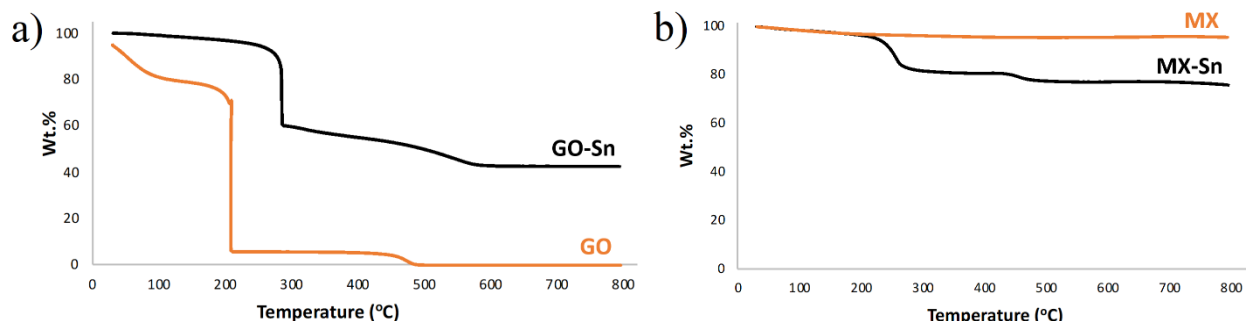


Figure 3.8 TGA analyses for GO/GO-Sn and MX/MX-Sn in air atmosphere.

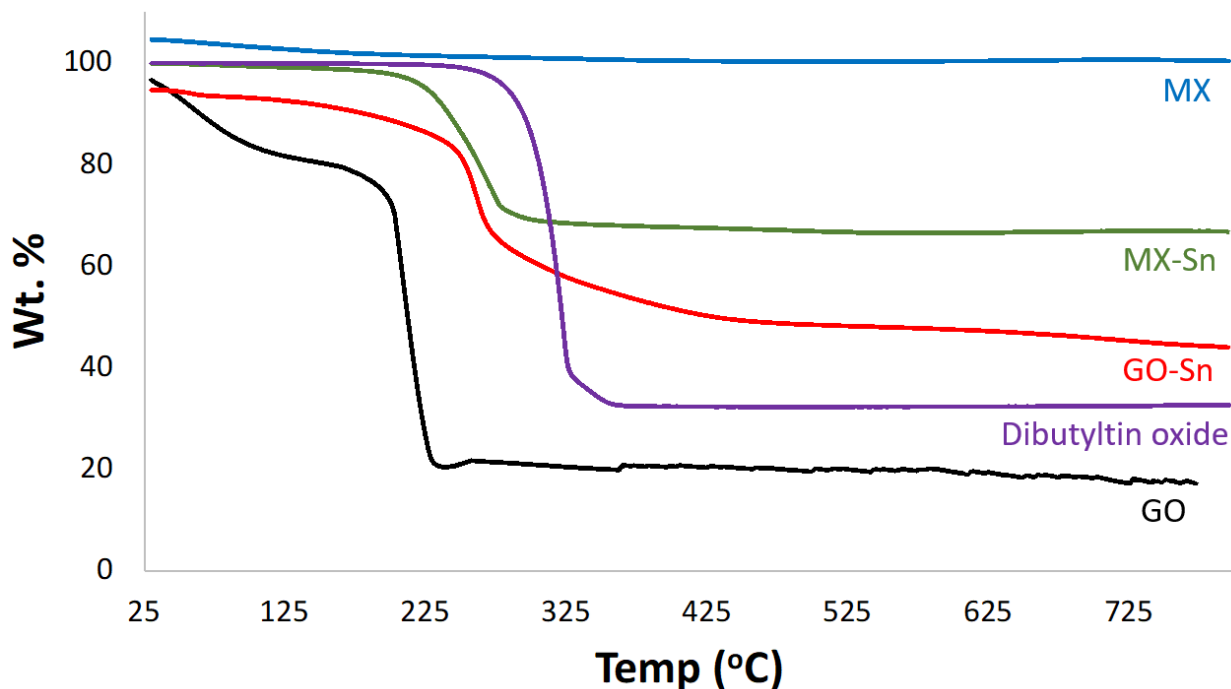


Figure 3.9 TGA analyses for GO, GO-Sn, MX, MX-Sn and Bu₂SnO in nitrogen atmosphere.

3.3 Transesterification of DMT and TMCD using 2D Heterogeneous Catalysts

The transesterification reaction was carried out using bulk melt method reported in literature [15]. As illustrated in Figure 3.10, the reaction setup included a three-neck round bottom 100 mL flask placed on a lower hemispherical heating mantle linked to J-KEM Scientific 260 instrument, in which its temperature monitoring probe was looped back into one of the flask necks. A Dean-Stark distillation receiver was connected to the middle neck using some grease to seal the joint, and a Graham condenser was placed on its top connected to cold water supply. 1 mol of dimethyl terephthalate (DMT) and 2 mol of 2,2,4,4-tetramethyl-1,3-cyclobutanediol (2 mol TMCD) were weighted and added to the flask. A small amount of methanol was also added to help the exfoliation of heterogeneous catalysts and immerse all reactants for better mixing. Considering the weight percent elemental tin is estimated to be about 33.4 % for GO-Sn and 67.8% for MX-Sn, the following equation was used to calculate the appropriate amount of catalyst to be added into the reaction (e.g. 200 ppm tin).

$$\text{tin loading (ppm)} = \frac{\text{elemental tin wt\%} \times \text{mass of catalyst}}{\text{mass of DMT} + \text{mass of TMCD} + \text{mass of catalyst}} \times 10^6$$

Once all reactants are in the flask, the remaining septum was capped with a rubber stopper after purging with nitrogen gas for few minutes. The thermostat on J-KEM instrument was set to a desired temperature depending on the experiment (e.g. 230 °C), and the reaction medium was allowed to reach this temperature. For the record, the initial time of reaction was measured from the moment the mixture reaches the desired temperature and the heat was maintained for 3 hours for the reaction to run. Meanwhile, a set of glass pipettes was pre-heated inside an oven at 200 °C to prevent sample from cooling down when transferring to a glass vial. As for the sampling, the rubber stopper was removed and roughly 1 mL of sample were pipetted to a glass vial, followed by quick purging with nitrogen gas and sealing with the rubber stopper.

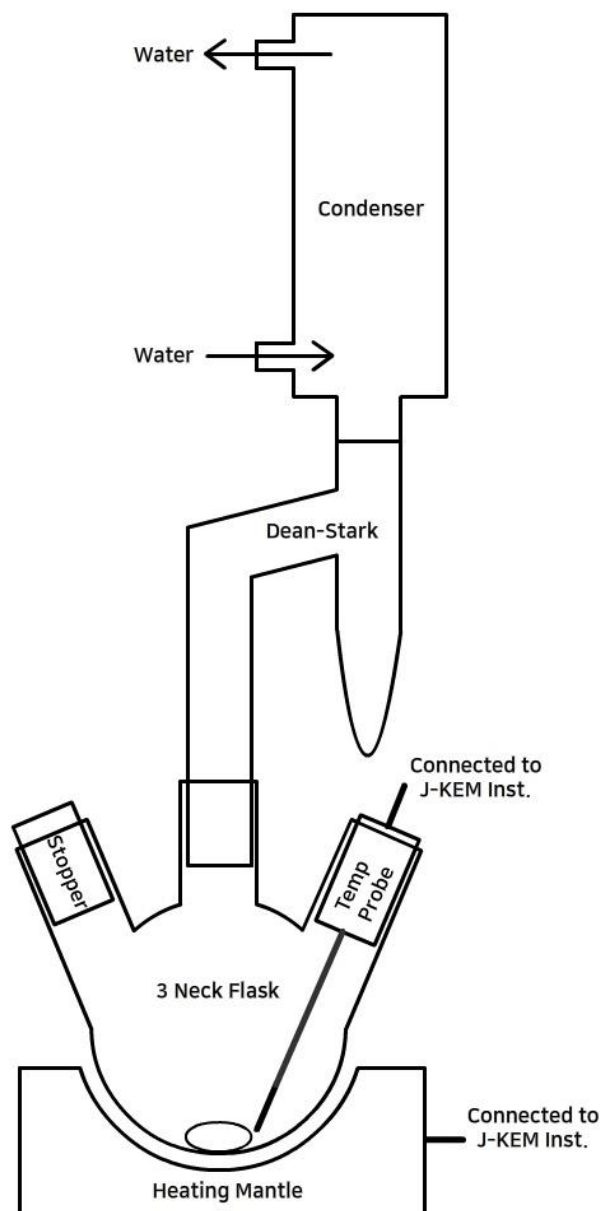


Figure 3.10 Lab-scale setup for transesterification reaction.

3.4 Transesterification Product Characterizations

The samples obtained from transesterification reactions were analyzed via Proton Nuclear Magnetic Resonance (^1H NMR) spectroscopy to determine the catalytic activities of 2D heterogeneous catalysts. As for NMR sample preparation, roughly 15 mg of a sample was completely dissolved in a glass vial filled with 1 mL of deuterated chloroform. A syringe attached with Sartorius MinisartTM 2.0 μm regenerated cellulose filter was used to remove any solid

particles from the sample solution, which was then pipetted to an NMR tube. Bruker Avance NEO 600 MHz NMR instrument at NC State METRIC facility was used with the following parameters: ^1H experiment, CDCl_3 solvent, 256 scans, and FID output. Then, the peaks observed in the spectrum data was analyzed with MestReNova (Mnova) software after setting tetramethylsilane (TMS) as the zero-point reference and necessary baseline correction. After correct assignment of the peaks, the calculations for percent DMT monomer conversion was carried out based on normalized amount of DMT aromatic protons and DMT methyl ester protons (an example NMR spectrum and the peak assignments shown in Appendix A).

The transesterification reactions between DMT and TMCD were conducted to monitor the catalytic activities and their dependence on different tin loading concentrations or reaction temperatures. Keeping the reaction temperature fixed at 230 °C, the effect of different tin loadings as a plot of percent DMT conversion versus reaction time is presented in Figure 3.11. Besides the noticeable error in few curves, generally the higher amount of both GO-Sn and MX-Sn catalysts seems to exhibit increased catalytic activities, maxing around the concentration of 300 ppm in both cases. Comparing the two catalysts, GO-Sn shows better kinetics at the similar tin loadings, where the percent conversion at initial 30-minute mark is overall higher than those of MX-Sn. Even at maximum 180-minute mark, GO-Sn tends to show slightly more stable results in terms of variance in percent conversions. While both have effectively catalyzed the transesterification reaction of DMT and TMCD at different loading conditions, GO-Sn was chosen as our primary target for further investigation based on these available data.

Choosing the middle ground of 200 ppm tin loading condition, the two additional studies on the catalytic behavior of GO-Sn catalyst are presented in Figure 3.12. The dependence of percent DMT conversion with respect to increasing reaction temperatures show a clear up-trend.

Not only do the initial 15-minute samples show significant jumps, but also the final 180-minute samples show expected increase of percent conversions as well. Furthermore, four repetitive reactions at 230 °C demonstrate acceptable reproducibility of the data with similar kinetics. All discussed percent conversion data and their numerical values are available in Appendix B.

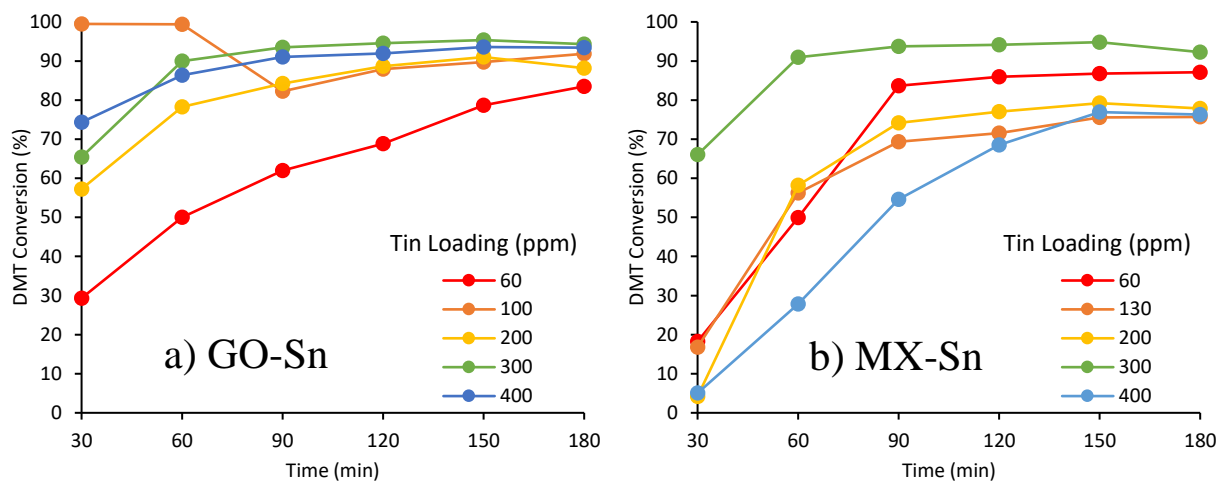


Figure 3.11 Percent DMT conversions of transesterification reactions between DMT and TMCD using GO-Sn or MX-Sn catalyst at different tin loadings.

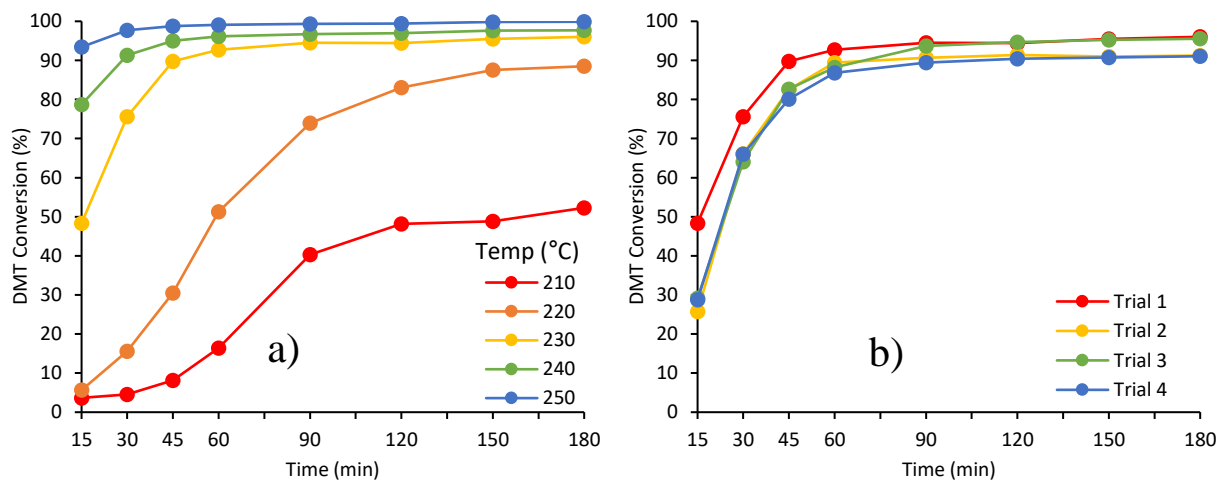


Figure 3.12 Percent DMT conversions of transesterification reactions between DMT and TMCD using GO-Sn catalyst (a) at different reaction temperatures and (b) from repetitive trials.

On the other hand, the physical appearances of the DMT/TMCD product sample have shown interesting results. In Figure 3.13, the blue borders indicate samples with percent DMT conversions below 50% whereas the green borders indicate above 50%. All samples below 50% conversions exhibit more of a paste-like consistency that are opaque and white in color, while the sample above 50% conversions are glass-like substance while being transparent and relatively brittle. It is not until the high temperature of 250 °C and beyond 120-minute mark that the samples begin to turn yellow in color. Possible reasoning behind this may be that GO component has degraded above its thermal limit or the leakage of air into the reaction flask during sampling has caused oxidation and eventually tinted the product yellow. From this understanding, transesterifications with GO-Sn catalyst produce the most desirable result at 200 ppm tin loading around 230 °C, so the future reactions with this catalyst will mainly use these two conditions.

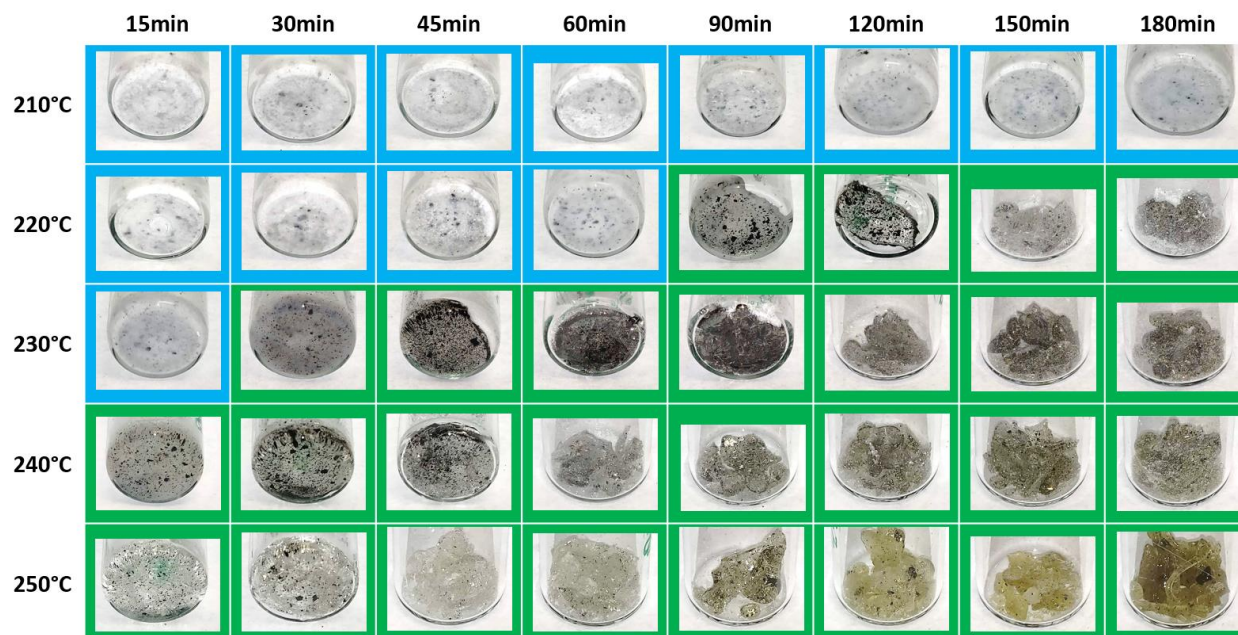


Figure 3.13 Physical appearances of DMT/TMCD/GO-Sn oligomer products depending on the reaction temperature and time.

Additionally, Inductively Coupled Plasma Mass Spectroscopy (ICP-MS) was used to study the concentration of elemental tin present in the final product samples. The oligomer samples were prepared from transesterification reactions between DMT and TMCD (1:2 molar ratio) using GO-Sn catalyst at two different tin loading concentrations: 200 ppm and 300 ppm. These reactions were running at 230 °C up to 3 hours, in which the samples were collected in hourly increments. After completely dissolving each sample in a small amount of acetone, the solution was run through a syringe attached with Sartorius Minisart™ 2.0 µm regenerated cellulose filter to collect filtrate on a watch glass. The solvent is then allowed to evaporate under the fume hood until a dried solid sample is obtained. Then, all samples were submitted to NC State CASL facility for the ICP-MS analysis.

Table 3.3 ICP-MS analyses of various samples to determine the amount of tin leaching (all samples are filtered unless stated otherwise).

Sample	Tin in Filtrate (ppm)	Tin Leached (%)
GO-Sn/DMT/TMCD, 300 ppm, 1 hr	16.98	5.7
GO-Sn/DMT/TMCD, 300 ppm, 2 hr	16.65	5.6
GO-Sn/DMT/TMCD, 300 ppm, 3 hr	3.92	1.3
GO-Sn/DMT/TMCD, 200 ppm, 1 hr	41.67	20.8
GO-Sn/DMT/TMCD, 200 ppm, 2 hr	12.62	6.3
GO-Sn/DMT/TMCD, 200 ppm, 3 hr	12.49	6.2
(A) GO-Sn/DMT/TMCD, 200 ppm, 3 hr, not filtered	158.97	79.5
(B) Bu ₂ SnO/DMT/TMCD, 200 ppm, no reaction	166.51	83.3
(C) GO-Sn/DMT/TMCD, 200 ppm, no reaction	38.80	19.4
(D) GO-Sn/Acetone	3.26 wt%	0.0039

The detected concentration of tin remaining in the filtered product and the percent tin leached from the initial GO-Sn catalyst are both reported in Table 3.3. As evident by rows 1-6, there is a small amount of leaching of tin from the GO matrix into the final product. Although there isn't notable difference between 200 ppm and 300 ppm tin loadings, the amount of tin leaching decreases as the reaction time increases. This is an unexpected outcome and one possible explanation could be that the longer heat exposure caused the GO flakes to somehow clump together and not pass through the filter membrane. This behavior may explain the lower tin leakage into filtrate and this part of the study is further discussed in the next section.

Similarly, four additional control samples were also submitted for ICP-MS analysis and listed in the same Table 3.3. The control sample **A** contained oligomer product from the transesterification reaction with GO-Sn/DMT/TMCD at 200 ppm for 3 hours, but not dissolved in solvent nor filtered at all. From the supposed 200 ppm tin loading, only 158.97 ppm were detected and this suggests that the actual weight percent tin grafted onto GO matrix is less than 33.4% from the preliminary TGA data. Performing back-calculation from the measured 158.97 ppm reveals that the estimated tin loading is 26.5% by weight. This ICP-MS data may be more reliable, because TGA calculation was based on the assumption of SnO₂ being the chemical structure left at the end of decomposition and this may not necessarily be true. Then, the comparison was made between sample **B** that contains filtered mixture of Bu₂SnO/DMT/TMCD at 200 ppm and sample **C** that contains filtered mixture of GO-Sn/DMT/TMCD/GO-Sn at 200 ppm. These two samples were simply stirred and dissolved in acetone to be filtered; thus, no heat was involved. The detected amount of tin from commercial Bu₂SnO catalyst was much higher than that of GO-Sn catalyst, suggesting that the GO matrix is partially retaining the tin species and prevents leakage into the filtrate. This is also confirmed by sample **D** that has filtrate collected from GO-Sn mixed in

acetone. The reported 3.26 wt% tin is only from 0.2 mg sample that actually made through the filter membrane. Based on the initial amount of tin from 500 mg GO-Sn mixed and this reported data, the calculation reveals that 0.0039% of tin actually leached from the matrix. Overall, there certainly is small amount of tin that gets leached into the product from the factors which are not entirely clear. However, this leached tin is no more than 5~20% of the initial amount grafted on GO sheets while the majority is being filtered out to mitigate any potential defects on the product.

3.5 Additional Characterizations of 2D Heterogeneous Catalysts

Both Scanning Electron Microscopy (SEM) and Energy-Dispersive X-ray Spectroscopy (EDX) were used to collect images and clarify any morphological changes happening to GO-Sn catalyst during the reaction. For SEM, control samples of plain GO nanosheet and the newly synthesized GO-Sn catalyst were submitted alongside few other treated samples. Two samples include GO-Sn vigorously stirred in acetone and methanol each for an hour and recovered. The other two samples include reacting GO-Sn (200 ppm tin loading) with DMT and TMCD at 230 °C for 1 and 3 hours. Then, the catalysts were recovered from the product via syringe filtration using Sartorius Minisart™ 2.0 µm regenerated cellulose filter. All six samples were observed using NC State AIF Verios 460L at 5,000x magnifications using the following parameters: voltage of 2.00 kV, current of 13 pA, working distance of ~5.0 mm, and tilt of 0 degrees.

As pictured in Figure 3.14, the pristine GO features a thin film with several wrinkles and crease across the surface. Unlike that of GO sample, the image of GO-Sn reveals large chunks of worm-like structures widely distributed throughout the surface. At a first glance, this appears to be embedded tin species because the only treatment made to GO sheet is the grafting of dibutyltin oxide. Even after being washed vigorously in acetone and methanol, these assumed-tin structures are still present on the surface of GO matrix. It is not until GO-Sn is used in the transesterification

reaction that those structures have disappeared or leached off, which is apparent in both 1-hour and 3-hour mark samples. The wrinkles of GO sheets are obstructed from view in samples **b**, **c**, and **d**, but are visible again in samples **e** and **f**. This evidently suggests that the assumed-tin moieties have detached from the surface, and they may have fallen off by either the heating process or the actual catalysis of DMT and TMCD.

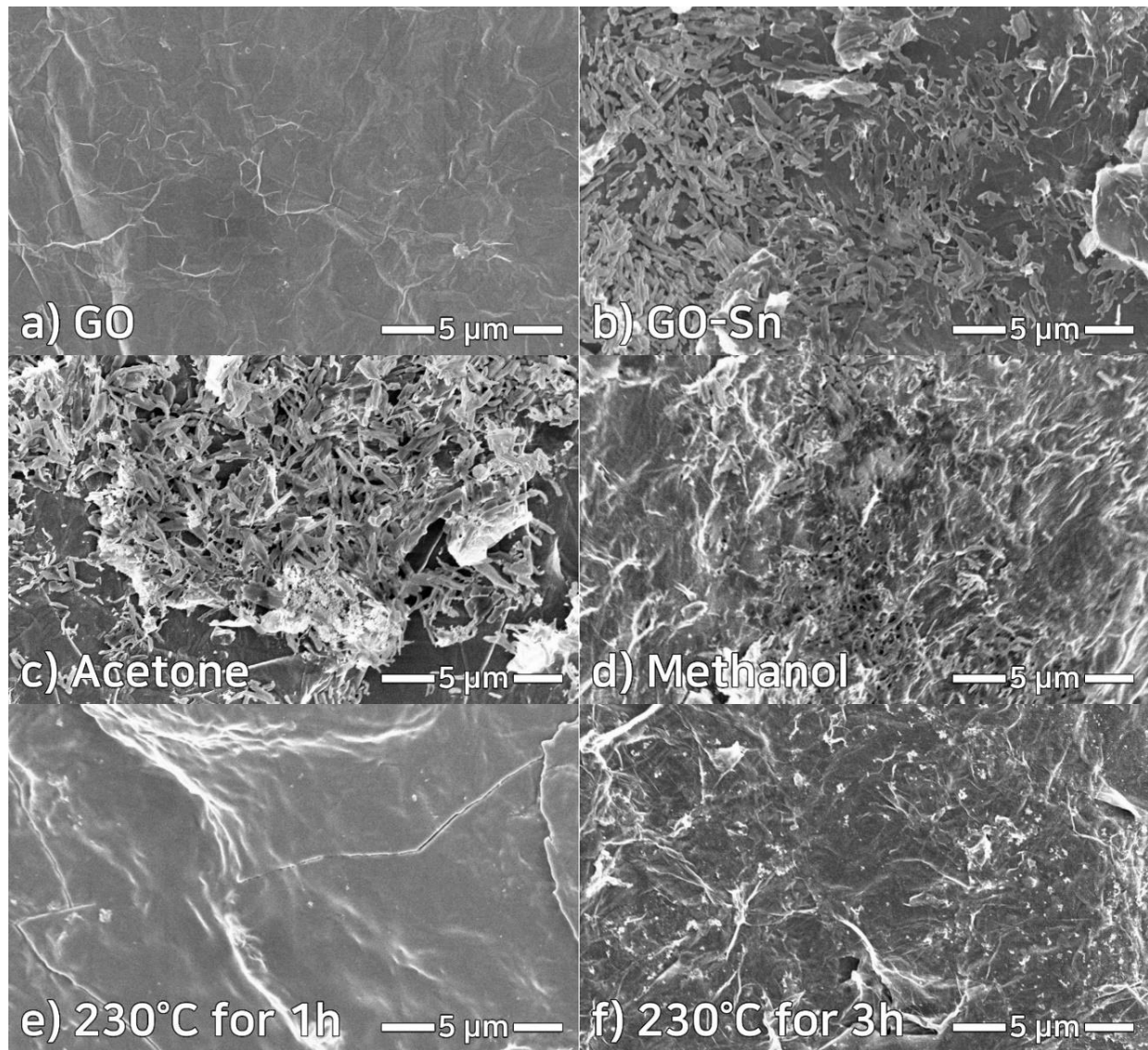


Figure 3.14 SEM images of GO and GO-Sn surfaces in various conditions.

Furthermore, Energy Dispersive X-ray Spectroscopy (EDX) was used to examine the unknown structures found on the surfaces of GO-Sn catalyst. This was done using NC State AIF Verios 460L with EDX detector at 5,000x magnification using the following parameters: voltage of 10.00 kV, current of 1.6 nA, working distance of ~5.2 mm, and tilt of 0 degrees. Figure 3.15 represents two distinctively different regions found on GO-Sn surface. The red region without any agglomerate species show 16.4 wt% tin whereas the green region focused on the assumed-tin structures show 35.2 wt% tin composition. This value is closely comparable to that of TGA data (33.4 wt% tin) which further supports the idea that the unknown substances are indeed tin compounds. The lower 16.4 wt% at the empty region could be explained by EDX being capable of detecting up to 1-2 μm in depth and the tin structures sandwiched in-between GO flakes are simply obstructed from the perceived view. However, this creates discrepancies with the ICP-MS data. Although the observed decreased leaching with the increased reaction time still remains elusive, GO-Sn composition of 26.5 wt% tin (ICP-MS) may be justified as the overall average of tin component while 35.2 wt% tin (EDX) is locally targeted on tin-rich region and does not represent the entirety of GO-Sn surface.

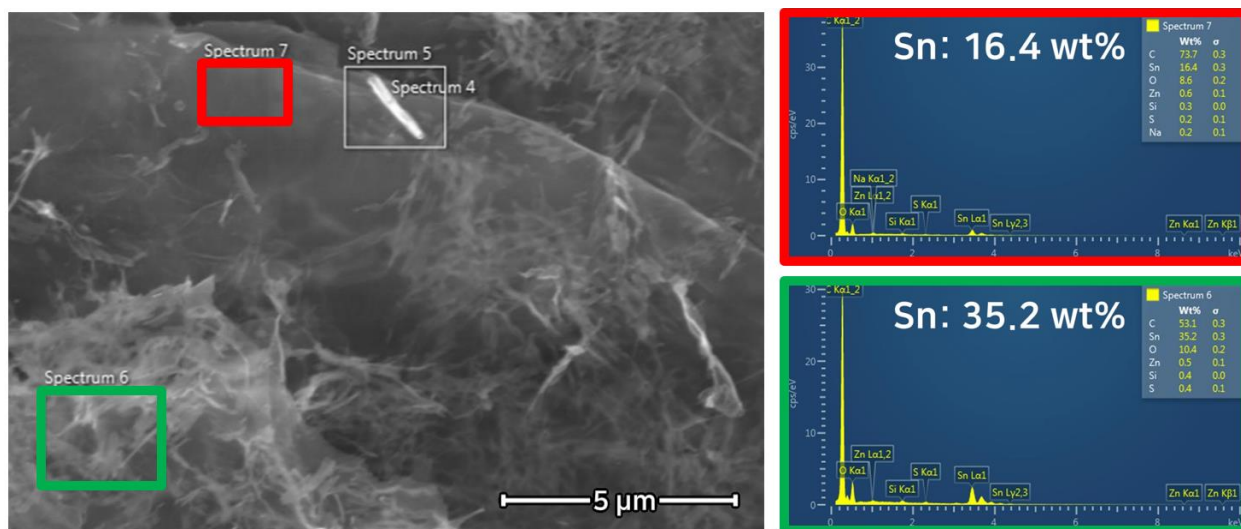


Figure 3.15 EDX image of GO-Sn surface to determine the percent weight of tin.

3.6 Experiments for Leaching and Reusability of 2D Heterogeneous Catalysts

The objective of developing the heterogeneous catalyst is to remove the catalytic moiety from the final product and mitigate potential issues caused by it. To investigate this matter, the separability of GO-Sn catalyst particles from the oligomer product is tested in two-way branched experiments as summarized in Figure 3.16. First, approximately 10 g of initial oligomer samples synthesized from DMT/TMCD/GO-Sn transesterification reactions (200 ppm tin loading and 230 °C for 3 hours) were fully dissolved in 300 mL of solvents including acetone, chloroform, and tetrahydrofuran (THF). Then, the mixtures were vacuum filtered using the setup illustrated by Figure 3.17 in order to obtain two key components: catalyst particles on the membrane filter and filtrate solution in the flask. In this small lab-scale filtration using 15 mm channel diameter connected to a typical fume hood's vacuum, the flowrate widely ranged from 1.2 mL/min (acetone) to 100 mL/min (THF) depending on the solvent used to dissolve the oligomer product, regardless of the difference in filter pore sizes (0.1 μm or 5.0 μm). After the filtration step, the catalyst particles were carefully recovered from the filter paper, whereas the filtrate solution was allowed to evaporate until dry solid samples were collected.

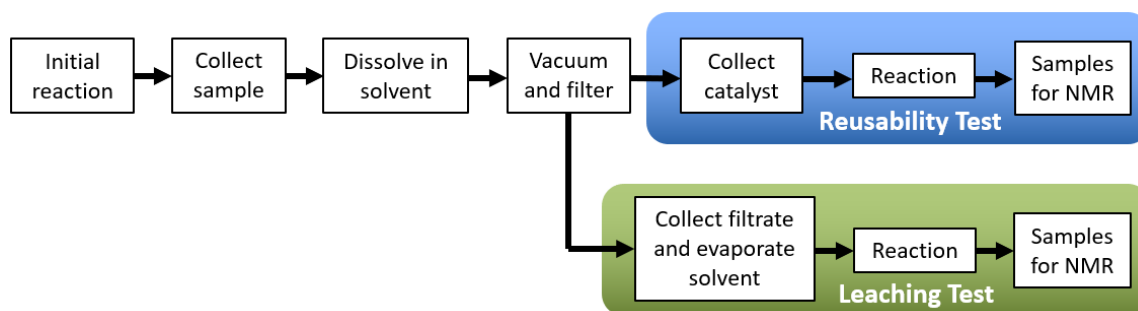


Figure 3.16 Summarized workflow of filtration experiments.

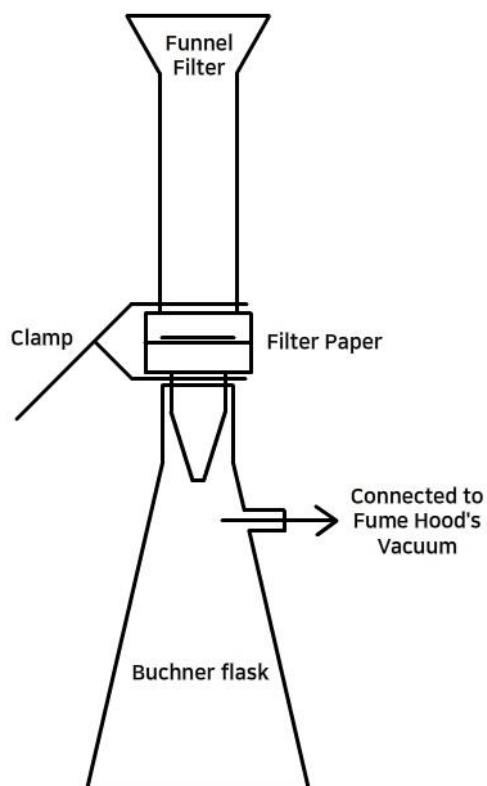


Figure 3.17 Lab-scale setup for catalyst filtration.

First, the dry filtrate was used to conduct the leaching test. If catalytic species have leached from the GO matrix during the initial reaction, it would have ended up in the filtrate and behaved like a homogeneous catalyst when used in a follow-up transesterification reaction. This in turn results in detectable amount of DMT monomer conversion. In order to test this, 6 g of the dry solids from filtrate, 2 g of new DMT, and 4 g of new TMCD reactants were heated at 230 °C for 3 hours without any additional catalyst. For the comparison purposes, NMR analyses have been conducted on the initial oligomer product before filtration, the obtained filtrate sample, the filtrate/DMT/TMCD sample at 60 °C (fully melted), and the filtrate/DMT/TMCD samples at 0-hour and 3-hour mark after reaching 230 °C. As evident from Table 3.4, both the initial product and the filtrate show similar percent conversions that suggest no significant impact from the filtration step. Upon adding new DMT and TMCD into the filtrate sample, DMT conversions are slashed to near 54-56% which is to be expected. The heating of mixtures for 3 hours shows an

increase in percent conversions for all samples, indicating that there was leaching of catalytic species into the final products. However, the varying extent of increased conversion across three filtration solvents suggests that the type of solvent plays a significant role on the amount of tin leaching. From the available data, calculations were made for percent conversions only accounting for the unreacted DMT (the last row). Out of the three, THF is the most preferable solvent for dissolving and filtering the oligomer product because the amount of tin leaching was the lowest with 29.9% DMT conversion; whereas, chloroform solvent leached the highest amount of tin and reflecting 59.2% DMT conversion.

Table 3.4 Percent DMT conversions of leaching experiment using three different solvents.

Sample	DMT Conversion (%)		
	Acetone	Chloroform	THF
Initial Product Before Filtration	93.6	94.6	94.6
Filtrate	93.7	94.4	94.8
Filtrate/DMT/TMCD, 60 °C	54.7	56.3	54.3
Filtrate/DMT/TMCD, 230 °C, 0 hr	53.5	56.4	54.7
Filtrate/DMT/TMCD, 230 °C, 3 hr	77.6	85.2	68.8
Solely Accounting for Unreacted DMT	46.8	59.2	29.9

As for the reusability test, the recovered catalysts from three different solvents were used again in a second transesterification reaction with the appropriate amounts of DMT/TMCD reactants to match 200 ppm tin loading. The reaction is carried out at 230 °C for 3 hours with 15-min incremental sampling for the first hour and 30-min incremental sampling for the rest 2 hours. The collected samples were again analyzed by NMR spectroscopy to calculate the percent DMT monomer conversions as shown in Figure 3.18. The data appears to be in alignment with the filtrate

leaching experiment, where the least leached catalyst recovered from THF solvent yields the highest catalytic activity, and the most leached one from chloroform is the least active of the three catalysts. Despite this, the overall performance of these recycled catalysts is relatively lower than that of 60 ppm GO-Sn (Figure 3.11a), suggesting that most of tin content responsible for the catalysis has been stripped off by either the heating process or the solvent. The discussed percent DMT conversion values are also available in Appendix B.

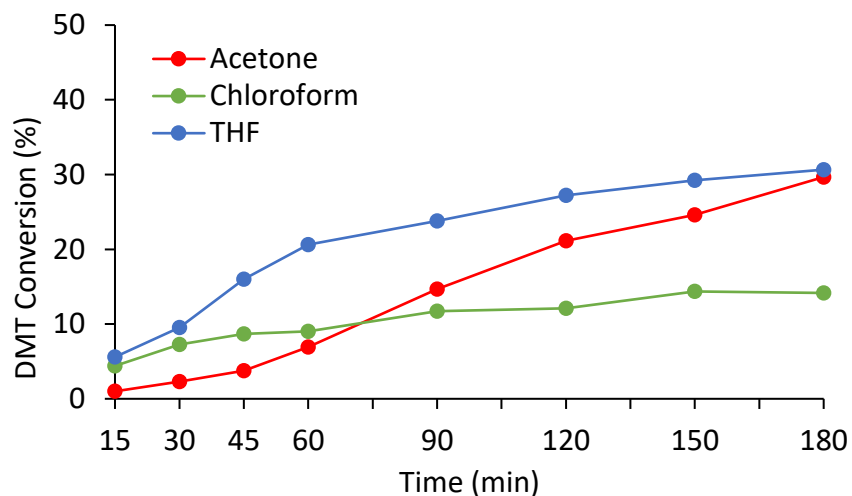


Figure 3.18 Percent DMT conversions of reusability experiment using three different solvents.

Accordingly, the previously proposed chemical structure of GO-Sn catalyst is modified to reflect the observed phenomena and discussions (Figure 3.19). Besides the expected butyltin oxide components grafted to GO matrix, there may also be butylamine attachments that trigger weak hydrophobic interaction with other dibutyltin oxide molecules and form agglomerates that can be easily fall off by the exposure to heat or solvent. If true, this supposedly explains the embedded structures on GO-Sn sheet from SEM images that have disappeared after reaction and solvent filtration (Figure 3.14).

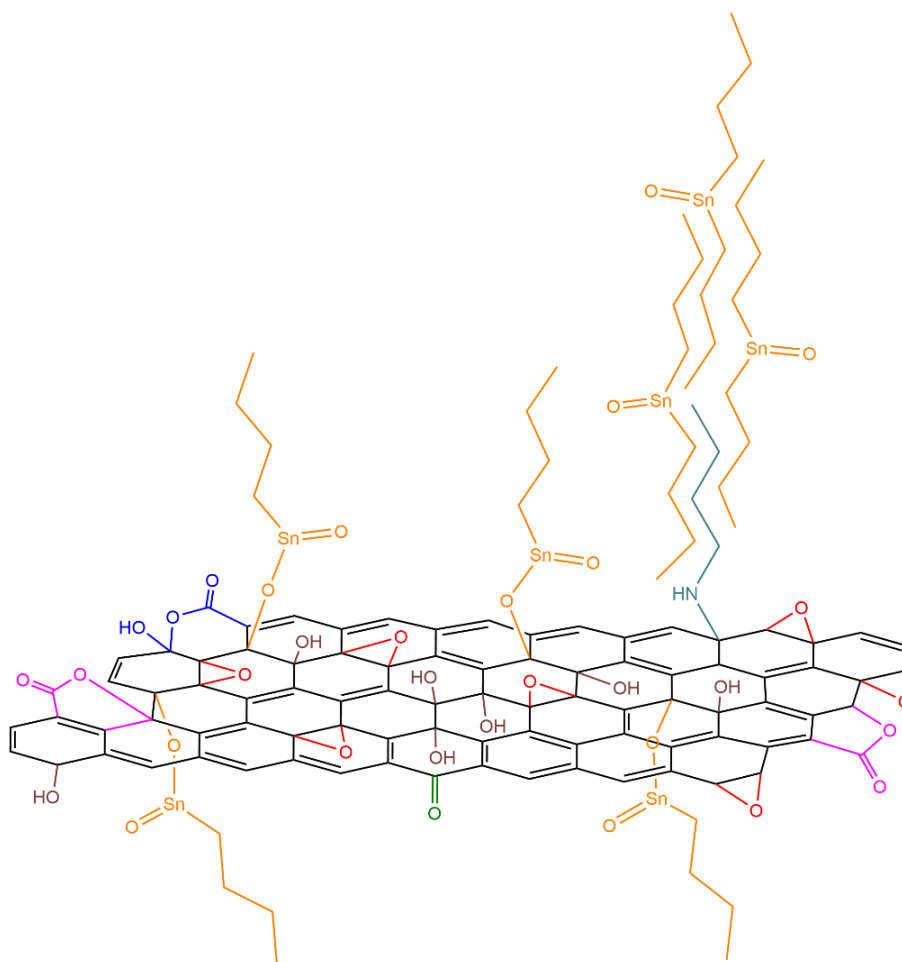


Figure 3.19 Modified chemical structure of GO-Sn catalyst.

3.7 Experiments for Alternative Monomers

In order to expand the understanding of catalytic activities against other reagents, GO-Sn has been used for transesterification reactions between DMT and a few commercially available diol-monomers. The reaction setup and procedures are the same as that of transesterification of DMT and TMCD with a few exceptions. 2 mol of ethylene glycol (EG), neopentyl glycol (NPG), 2-methyl-1,3-propanediol (MPD), and 1,4-cyclohexanedimethanol (CHDM) have been individually tested with 1 mol of DMT and GO-Sn (200 ppm tin loading) at 230 °C for 3 hours. Methanol was excluded for the reactions with EG and MPD as they are already in a liquid state at room temperature unlike the others. In this scenario, only one sample was taken at the end of 3-

hour mark for each reaction, and they were analyzed via NMR for the percent DMT monomer conversions as shown in Table 3.5. Interestingly, GO-Sn is highly capable of catalyzing transesterification reactions between DMT and other diol monomers, with the exception of EG. Despite having primary alcohols with the least steric hindrance out of all reactants, the reactions between DMT and EG did not show high percent conversions in two different trials. Noting that a transesterification reaction is a reversible process, it may be that EG has found the equilibrium at the point of 53~60% DMT conversion, but it still remains unclear what exactly caused this outlier.

Table 3.5 Transesterification reactions between DMT and different diols using GO-Sn catalyst.

Diol Reagent	2 mol Diol (g or mL)	1 mol DMT (g)	GO-Sn (mg)	Methanol (mL)	DMT Conv. (%)
TMCD	7.5 g	5.0	7.5	15	94.6
EG	4.1 mL	7.0	6.9	-	59.7; 52.8
NPG	6.4 g	6.0	7.4	12	96.8
MPD	5.5 mL	6.0	6.9	-	98.6
CHDM	8.9 g	6.0	8.9	12	97.9

CHAPTER 4: Conclusions

In summary, new heterogeneous catalysts based on two-dimensional matrices have been developed and characterized. By grafting a conventional dibutyltin oxide catalyst on the surface of graphene oxide and MXene nanosheets, these new solid-supported species behave as heterogeneous catalysts that effectively catalyze transesterification reactions between dimethyl terephthalate and a number of diol monomers. Evidently, the percent DMT monomer conversions are reasonably high with the appropriate amount of tin loading and temperature in lab-scale reactions, providing a promising solution to polymerization reactions in industrial settings. Furthermore, partial separations of these catalytic species from the reaction products have been demonstrated via lab scale vacuum filtration processes. This provides a vital step to mitigate any potential defects in the final product due to the remnants of active catalysts. However, the catalysts are not without their flaws, and their noted tin leaching and reusability issues may be addressed in future work by thermally treating the catalytic components, optimizing the reaction protocols, or exploring different linkers to create heterogeneous catalysts in a similar manner. On a final note, this confidential project in collaboration with Eastman Chemical Company demonstrated that the chemical grafting of dibutyltin oxide on the 2D surfaces of GO and MX produces an exceptional result of working heterogeneous catalysts; paving a novel method of transesterification synthesis.

REFERENCES

1. Román-Martínez, M. C.; Salinas-Martínez de Lecea, C. Heterogenization of Homogeneous Catalysts on Carbon Materials. In *New and Future Developments in Catalysis*; Elsevier, 2013; pp 55-78.
2. Matyjaszewski, K.; Pintauer, T.; Gaynor, S. Removal of Copper-Based Catalyst in Atom Transfer Radical Polymerization Using Ion Exchange Resins. *Macromolecules* **2000**, *33* (4), 1476-1478.
3. Trimm, D. L. The Regeneration or Disposal of Deactivated Heterogeneous Catalysts. *Applied Catalysis A: General* **2001**, *212* (1-2), 153-160.
4. Crabtree, R. H. *The Organometallic Chemistry of the Transition Metals*, 6th ed.; John Wiley & Sons, Inc., 2014.
5. Cornils, B.; Börner, A.; Franke, R.; Zhang, B.; Wiebus, E.; Schmid, K. Hydroformylation. In *Applied Homogeneous Catalysis with Organometallic Compounds*; Wiley-VCH Verlag GmbH & Co. KGaA, 2017; pp 23–90.
6. Denisov, E. T.; Sarkisov, O. M.; Likhtenshtein, G. I. Catalysis by Metal Complexes. In *Chemical Kinetics*; Elsevier, 2003; pp 472–501.
7. Bhaduri, S.; Mukesh, D. *Homogeneous Catalysis*, 2nd ed.; John Wiley & Sons, Inc., 2014.
8. Pang, K.; Kotek, R.; Tonelli, A. Review of Conventional and Novel Polymerization Processes for Polyesters. *Progress in Polymer Science* **2006**, *31* (11), 1009–1037.
9. Ali, M. E.; Rahman, M. M.; Sarkar, S. M.; Hamid, S. B. A. Heterogeneous Metal Catalysts for Oxidation Reactions. *Journal of Nanomaterials* **2014**, *1*, 1-23.

10. Zhang, M.; Moore, R. B.; Long, T. E. Melt Transesterification and Characterization of Segmented Block Copolyesters Containing 2,2,4,4-Tetramethyl-1,3-Cyclobutanediol. *J. Polym. Sci. A Polym. Chem.* **2012**, *50* (18), 3710-3718.
11. Ferreira, A. B.; Lemos Cardoso, A.; da Silva, M. J. Tin-Catalyzed Esterification and Transesterification Reactions: A Review. *ISRN Renewable Energy* **2012**, 1-13.
12. Nagahata, R.; Sugiyama, J.-I.; Goyal, M.; Asai, M.; Ueda, M.; Takeuchi, K. Solid-Phase Thermal Polymerization of Macrocyclic Ethylene Terephthalate Dimer Using Various Transesterification Catalysts. *J. Polym. Sci. A Polym. Chem.* **2000**, *38* (18), 3360-3368.
13. Quisenberry, R. K. Segmented copolyester of 2, 2, 4, 4-tetramethyl-1, 3-cyclobutylene terephthalate and ethylene terephthalate. US3249652A, May 3, 1966.
14. Ltd., K. Improved linear polyesters. GB1044015A, September 28, 1966.
15. Kelsey, D. R.; Scardino, B. M.; Grebowicz, J. S.; Chuah, H. H. High Impact, Amorphous Terephthalate Copolyesters of Rigid 2,2,4,4-Tetramethyl-1,3-cyclobutanediol with Flexible Diols. *Macromolecules* **2000**, *33* (16), 5810-5818.
16. Meneghetti, M. R.; Meneghetti, S. M. P. Sn(IV)-Based Organometallics as Catalysts for the Production of Fatty Acid Alkyl Esters. *Catal. Sci. Technol.* **2015**, *5* (2), 765-771.
17. Liang, Y.; Su, K.; Cao, L.; Gao, Y.; Li, Z. Study on the Transesterification and Mechanism of Bisphenol A and Dimethyl Carbonate Catalyzed by Organotin Oxide. *Chem. Pap.* **2019**, *73* (9), 2171-2182.
18. Ali, B.; Yusup, S.; Quitain, A. T.; Alnarabiji, M. S.; Kamil, R. N. M.; Kida, T. Synthesis of Novel Graphene Oxide/Bentonite Bi-Functional Heterogeneous Catalyst for One-Pot

- Esterification and Transesterification Reactions. *Energy Conversion and Management* **2018**, *171*, 1801-1812.
19. Thomas, J. M.; Thomas, W. J. *Principles and Practice of Heterogeneous Catalysis*, 2nd ed.; Wiley-VCH Verlag GmbH & Co. KGaA, 2015.
20. Rothenberg, G. *Catalysis*; Wiley-VCH Verlag GmbH & Co. KGaA, 2008.
21. Singh, A. K.; Fernando, S. D. Reaction Kinetics of Soybean Oil Transesterification Using Heterogeneous Metal Oxide Catalysts. *Chem. Eng. Technol.* **2007**, *30* (12), 1716-1720.
22. Singh, A. K.; Fernando, S. D. Transesterification of Soybean Oil Using Heterogeneous Catalysts. *Energy Fuels* **2008**, *22* (3), 2067–2069.
23. Ramachandran, K.; Suganya, T.; Nagendra Gandhi, N.; Renganathan, S. Recent Developments for Biodiesel Production by Ultrasonic Assist Transesterification Using Different Heterogeneous Catalyst: A Review. *Renewable and Sustainable Energy Reviews* **2013**, *22*, 410–418.
24. Aransiola, E. F.; Ojumu, T. V.; Oyekola, O. O.; Madzimbamuto, T. F.; Ikhu-Omoregbe, D. I. O. A Review of Current Technology for Biodiesel Production: State of the Art. *Biomass and Bioenergy* **2014**, *61*, 276-297.
25. Kumar, D.; Ali, A. Transesterification of Low-Quality Triglycerides over a Zn/CaO Heterogeneous Catalyst: Kinetics and Reusability Studies. *Energy Fuels* **2013**, *27* (7), 3758-3768.
26. Ilgen, O. Dolomite as a Heterogeneous Catalyst for Transesterification of Canola Oil. *Fuel Processing Technology* **2011**, *92* (3), 452-455.

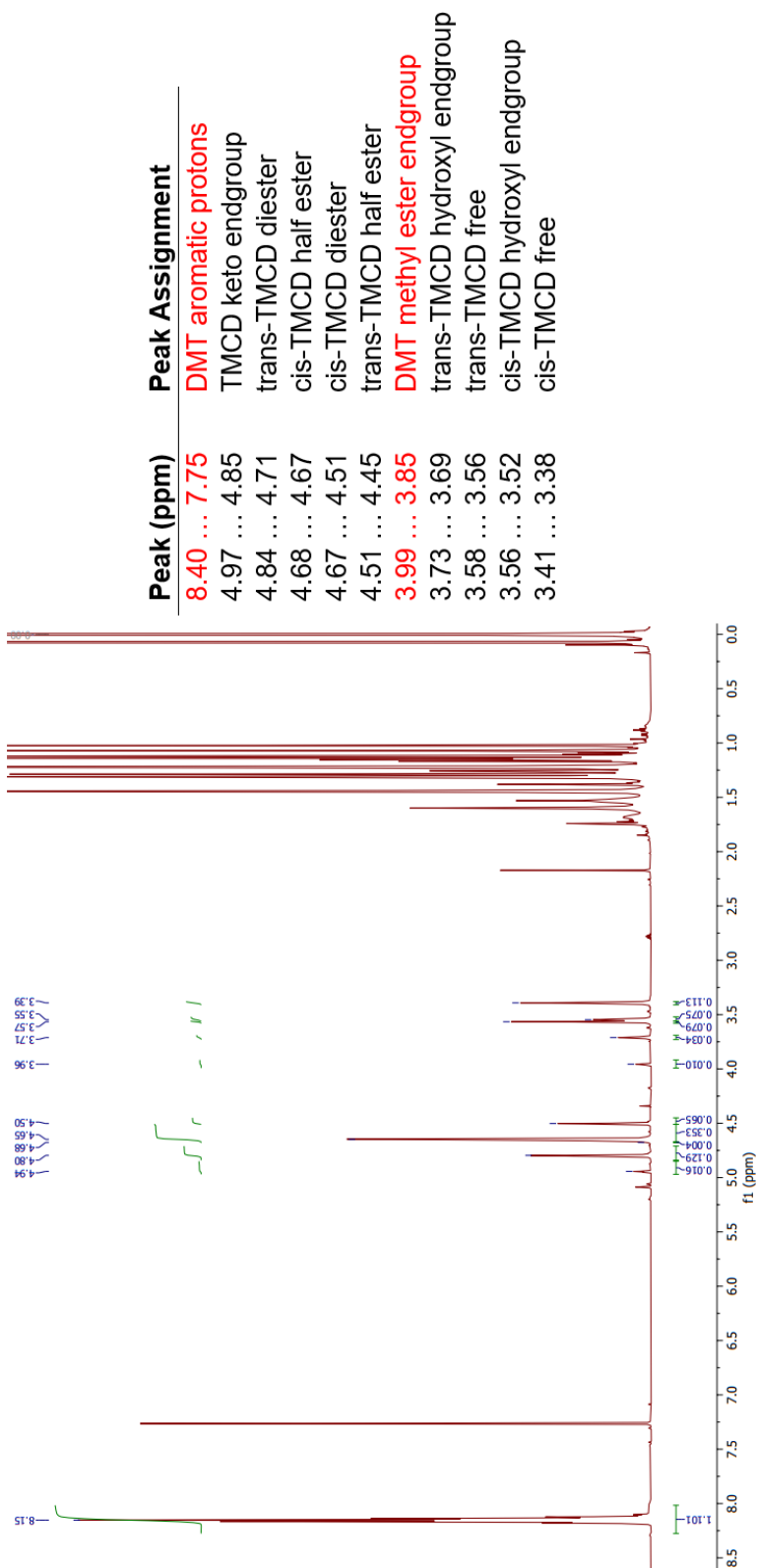
27. Meyer, U.; Hoelderich, W. F. Transesterification of Methyl Benzoate and Dimethyl Terephthalate with Ethylene Glycol over Basic Zeolites. *Applied Catalysis A: General* **1999**, *178* (2), 159-166.
28. Soldano, C.; Mahmood, A.; Dujardin, E. Production, Properties and Potential of Graphene. *Carbon* **2010**, *48* (8), 2127-2150.
29. Kuila, T.; Bose, S.; Mishra, A. K.; Khanra, P.; Kim, N. H.; Lee, J. H. Chemical Functionalization of Graphene and Its Applications. *Progress in Materials Science* **2012**, *57* (7), 1061-1105.
30. Singh, V.; Joung, D.; Zhai, L.; Das, S.; Khondaker, S. I.; Seal, S. Graphene Based Materials: Past, Present and Future. *Progress in Materials Science* **2011**, *56* (8), 1178-1271.
31. Gogotsi, Y.; Anasori, B. The Rise of MXenes. *ACS Nano* **2019**, *13* (8), 8491-8494.
32. Lei, J.-C.; Zhang, X.; Zhou, Z. Recent Advances in MXene: Preparation, Properties, and Applications. *Front. Phys.* **2015**, *10* (3), 276-286.
33. Hummers Jr., W. S.; Offeman, R. E. Preparation of Graphitic Oxide. *J. Am. Chem. Soc.* **1958**, *80* (6), 1339.
34. Tontini, G.; Greaves, M.; Ghosh, S.; Bayram, V.; Barg, S. MXene-Based 3D Porous Macrostructures for Electrochemical Energy Storage. *J. Phys. Mater.* **2020**, *3* (2), 1-31.
35. Lim, H. N.; Huang, N. M.; Loo, C. H. Facile Preparation of Graphene-Based Chitosan Films: Enhanced Thermal, Mechanical and Antibacterial Properties. *Journal of Non-Crystalline Solids* **2012**, *358* (3), 525-530.

36. Loy, A. C. M.; Quitain, A. T.; Lam, M. K.; Yusup, S.; Sasaki, M.; Kida, T. Development of High Microwave-Absorptive Bifunctional Graphene Oxide-Based Catalyst for Biodiesel Production. *Energy Conversion and Management* **2019**, *180*, 1013-1025.
37. Gaidukevič, J.; Barkauskas, J.; Malaika, A.; Rechnia-Gorący, P.; Możdyńska, A.; Jasulaitienė, V.; Kozłowski, M. Modified Graphene-Based Materials as Effective Catalysts for Transesterification of Rapeseed Oil to Biodiesel Fuel. *Chinese Journal of Catalysis* **2018**, *39* (10), 1633-1645.
38. Xu, Z.; Peng, L.; Liu, Y.; Liu, Z.; Sun, H.; Gao, W.; Gao, C. Experimental Guidance to Graphene Macroscopic Wet-Spun Fibers, Continuous Papers, and Ultralightweight Aerogels. *Chem. Mater.* **2016**, *29* (1), 319-330.
39. Alhabeb, M.; Maleski, K.; Anasori, B.; Lelyukh, P.; Clark, L.; Sin, S.; Gogotsi, Y. Guidelines for Synthesis and Processing of Two-Dimensional Titanium Carbide (Ti₃C₂T_x MXene). *Chem. Mater.* **2017**, *29* (18), 7633-7644.

APPENDICES

Appendix A

An Example NMR Spectrum of DMT/TMCD/GO-Sn 200 ppm at 230 °C for 3 hours



Appendix B

Percent Conversions of DMT/TMCD and GO-Sn at Different Tin Loadings

Tin Loading (ppm)	DMT Conversion (%)					
	30 min	60 min	90 min	120 min	150 min	180 min
60	29.33	50.12	61.98	68.82	78.69	83.50
100	99.49	99.42	82.25	87.89	89.71	91.86
200	57.26	78.28	84.28	88.68	91.01	88.16
300	65.43	90.05	93.47	94.58	95.36	94.34
400	74.33	86.36	91.03	91.97	93.58	93.45

Percent Conversions of DMT/TMCD and MX-Sn at Different Tin Loadings

Tin Loading (ppm)	DMT Conversion (%)					
	30 min	60 min	90 min	120 min	150 min	180 min
60	18.25	49.94	83.71	85.93	86.79	87.13
130	16.82	56.24	69.31	71.53	75.55	75.69
200	4.20	58.19	74.18	77.02	79.22	77.88
300	66.03	90.98	93.76	94.11	94.82	92.30
400	5.05	27.80	54.58	68.51	76.93	76.28

Percent Conversions of DMT/TMCD and GO-Sn at Different Reaction Temperatures

Temp (°C)	DMT Conversion (%)							
	15 min	30 min	45 min	60 min	90 min	120 min	150 min	180 min
210	3.67	4.55	8.16	16.41	40.31	48.16	48.81	52.28
220	5.65	15.63	30.52	51.25	73.94	83.06	87.55	88.50
230	48.35	75.58	89.78	92.69	94.49	94.37	95.46	96.03
240	78.71	91.29	95.04	96.18	96.69	96.93	97.61	97.70
250	93.43	97.67	98.78	99.08	99.35	99.41	99.83	99.89

Percent Conversions of DMT/TMCD/GO-Sn, 200 ppm, 230 °C, for Four Repetitive Trials

Trial	DMT Conversion (%)							
	15 min	30 min	45 min	60 min	90 min	120 min	150 min	180 min
1st	48.35	75.58	89.78	92.69	94.49	94.37	95.46	96.03
2nd	25.76	66.07	82.56	89.43	90.69	91.38	91.02	91.27
3rd	29.17	64.07	82.62	88.24	93.68	94.64	95.22	95.54
4th	28.80	65.99	80.12	86.78	89.42	90.39	90.76	91.06

Percent Conversions of DMT/TMCD and recovered GO-Sn, 200 ppm, 230 °C

Solvent	DMT Conversion (%)							
	15 min	30 min	45 min	60 min	90 min	120 min	150 min	180 min
Acetone	1.01	2.31	3.74	6.91	14.68	21.16	24.62	29.67
Chloroform	4.40	7.27	8.69	9.01	11.72	12.11	14.36	14.18
THF	5.59	9.53	16.01	20.63	23.81	27.22	29.23	30.66